

DISSERTATION

BIG FISH START SMALL

Submitted by

Clinton Leach

Graduate Degree Program in Ecology

In partial fulfillment of the requirements

For the Degree of Doctor of Philosophy

Colorado State University

Fort Collins, Colorado

Spring 2020

Doctoral Committee:

Advisor: Colleen Webb

LeRoy Poff

Barry Noon

Mevin Hooten

Copyright by Clinton Leach 2020

All Rights Reserved

ABSTRACT

BIG FISH START SMALL

Individuals of the same species often participate in substantially different predator-prey interactions. In many species, these differences are driven by individual size and the ontogenetic niche shifts that occur as an individual grows. This intraspecific size-structure can have profound consequences for our understanding of food web structure and community dynamics. These consequences are particularly important in exploited marine ecosystems where fisheries often target the largest individuals and size-structured feedbacks have been implicated in preventing collapsed fisheries from recovering. In this dissertation, we explored the consequences of this size-structure for the Scotian Shelf and Gulf of Alaska ecosystems. To understand how the collapse of the cod stock on the Scotian Shelf may have fed back on the demographic landscape of cod, we developed a model to estimate how the length-dependent growth and survival of cod changed before and after the collapse. We found that forage fish, released from top-down control, likely played an important role in limiting cod access to food, with consequences for cod survival and the potential for long term recovery. To better understand the community context of these changes, we developed a multivariate autoregressive model to capture how shifts in species' size distributions may have driven changes in the interspecific interaction landscape on the Scotian Shelf. This study found further evidence for the role of forage fish in preventing cod recovery, and linked the corresponding changes in interaction structure to an increase in the overall instability of the system. Lastly, we explored the community structure of ontogenetic niche shifts in the Gulf of Alaska by developing a model to identify trophic groups – collections of individuals with similar interaction patterns – in an individual-level food web assembled from stomach contents data. The identified trophic groups revealed substantial overlap in the ontogenetic trajectories of Gulf of Alaska predator species and the low-dimensional structure of the individual-level food web. This work represents a step toward

incorporating individual-level processes into modeling frameworks that can be used to both inform existing theory with data and to inform fisheries management. Specifically, this research highlights the different trophic roles that individuals of a species occupy as they grow, and the importance of growth in moving individuals up the food web and maintaining community structure and stability. Our findings suggest that disruptions to this flow and the resulting loss of large individuals can generate a cascade of effects through the system, leading to fundamental reorganization and increased instability.

ACKNOWLEDGEMENTS

First of all, I would like to thank my committee, LeRoy Poff, Barry Noon, and Mevin Hooten, for their guidance and feedback. Funding for this work was provided in part by the NSF Graduate Research Fellowship Program and Graduate Research Opportunities Worldwide under grant DGE-1321845, and the NSF Marine Resources Research Coordination Network under grant number 1140207. I would like to thank Martin Hartvig and Ken Andersen for hosting me during my GROW fellowship in Denmark and for contributions to the development of Chapter 2. I would also like to thank Ken Frank from DFO Canada for providing the Scotian Shelf data and related feedback, as well as Kerim Aydin from the Alaska Fisheries Science Center at NOAA for providing the Gulf of Alaska stomach contents data. Without the space, time, and support provided by CSU Writes, none of this would have been written on anything close to the required time scale. I am deeply grateful for the feedback, support, and friendship of the Webb lab (including Greg Ames, Andrew Kanarek, Michael Buhnerkempe, Dan Grear, Sarah Pabian, Kim Pepin, Angie Luis, Dave Hayman, Kim Tsao, Nels Johnson, Clay Hallman, Erin Gorsich, Ryan Miller, Tatiana Xifara, E Schlatter, Gabe Gellner, Mark Wilbur, Deedra Murrieta, Clif McKee, Ben Golas, Lindsay Beck-Johnson, Katie Owers, Brooke Berger, Kendra Gilbertson, Rachel Oidtman, and Tanya Dewey), who consistently made it a pleasure to come to work every day and whose company I do and will miss. I also need to thank my parents Scott and Sandy Leach for, well, everything. And lastly, I would like to thank my advisor Colleen Webb for putting up with me for 9 years, for keeping me motivated and excited (to the extent possible) about science, for the insight and feedback and generosity and friendship, and for generally being an excellent advisor.

DEDICATION

To Scott and Sandy Leach, my parents and roommates. You have been, and always shall be, my friends.

TABLE OF CONTENTS

ABSTRACT	ii
ACKNOWLEDGEMENTS	iv
DEDICATION	v
LIST OF TABLES	viii
LIST OF FIGURES	ix
Chapter 1 Introduction	1
Chapter 2 The changing demographic landscape of Scotian Shelf cod	6
2.1 Introduction	6
2.2 Methods	8
2.2.1 Data model	9
2.2.2 Chew-chew train process model	10
2.2.3 Parameterization and priors	12
2.2.4 Implementation and sampling	14
2.2.5 Evaluating long-term population growth and sensitivity	14
2.3 Results	15
2.4 Discussion	17
2.4.1 Feedbacks	26
2.4.2 Conclusions	27
Chapter 3 The changing interaction landscape of the Scotian Shelf fish community	28
3.1 Introduction	28
3.2 Methods	30
3.2.1 Data	30
3.2.2 Data model	31
3.2.3 MAR del mar	31
3.2.4 Gaussian process regression for interaction matrices	32
3.2.5 Implementation	33
3.2.6 Stability analysis	33
3.3 Results	34
3.4 Discussion	35
3.4.1 Summary	35
3.4.2 Trophic cascade and loss of top-down control	41
3.4.3 System stability	42
3.4.4 Cod recovery and management	44
3.4.5 Future work	45
3.4.6 Conclusions	46

Chapter 4	Food web structure of ontogenetic niche shifts	47
4.1	Introduction	47
4.2	Methods	49
4.2.1	Stomach contents data	49
4.2.2	Bento box process model	50
4.2.3	Priors	52
4.2.4	Implementation	52
4.3	Results	53
4.4	Discussion	55
4.4.1	Summary	55
4.4.2	The structure of the ontogenetic niche space	58
4.4.3	Extensions and future work	63
4.4.4	Conclusions	64
Chapter 5	Conclusion	66
Bibliography	69
Appendix	84
Chapter 2 supplemental material	84
Full model	84
Calculation of λ_{it}	85
Chapter 3 supplemental material	88
Full model	88
Chapter 4 supplemental material	89
Full model	89

LIST OF TABLES

2.1	Model parameters, their description, and their values.	13
-----	--	----

LIST OF FIGURES

2.1	Length-at-age data and model predictions. The points represent the observed average length as a function of age, and the gray ribbon represents the posterior 95% credible interval of the w_{at}	18
2.2	Catch-at-length data and model predictions. The points represent the observed average abundance per trawlable unit in 3cm length bins, and the gray ribbon represents the posterior 95% credible interval of the catchability-scaled λ_{it}	19
2.3	Estimated growth and survival trajectories for different sizes of cod through time. The panels on the left show estimated 6 month growth increments. The panels on the right show the estimated 6 month survival probabilities. The black line indicates the posterior median, while the gray ribbon represents the posterior 95% credible interval. The dashed line indicates 1993, the year the cod fishery was closed.	20
2.4	Projected spawning stock biomass 20 years ahead as a function of the initial year of the simulation, where growth and survival regimes were held constant at that year's values. The black points indicate the posterior median, while the gray lines indicate the 95% credible interval.	21
2.5	Heatmap of long-term spawning stock biomass predicted by simulating the population ahead 20 years from 2003, given growth and survival regimes fixed at their values in the given years. The dark blue regions correspond to demographic regimes predicted to lead to local extinction. The vertical banding of these regions indicates survival regimes for which no observed growth regime could prevent the predicted local extinction.	22
2.6	The scaled sensitivity of the projected spawning stock biomass 20 years ahead from 2003 to the growth (left) and survival (right) process convolution parameters located at the given size (i.e., $\partial SSB_{2023} / \partial \epsilon_k$, scaled by SSB_{2023} , where ϵ_k is located at length u_k) The points give the posterior median, while the lines give the posterior 95% credible intervals.	23
3.1	Abundance and average length trajectories for cod, haddock, herring, and sand lance. Left: the points indicate observed abundance (the y_{it}), the solid black line indicates the posterior median predicted abundance, and the gray ribbon indicates the 90% posterior credible interval. The dashed line represents the posterior median predictions holding B constant at its value in 1986, when average cod length was largest. Right: the points indicate the observed average length and the black line indicates the <i>a priori</i> smoothed estimate (used to populate x).	36
3.2	The posterior mean interaction surface as a function of the average length of the two species involved. The x-axis gives the average length of the source species (i.e., the species doing the influencing), and the y-axis gives the average length of the target species (i.e., the species being influenced). The arrows demonstrate the shift of the cod-sand lance interactions from 1986, the year of maximum average cod length, to 2002, the year of minimum average cod length. The solid line represents the effect of cod on sand lance, while the dashed line represents the effect of sand lance on cod.	37

3.3	Snapshots of the interaction structure in 1986 (the year of maximum cod average length), and 2002 (the year of minimum cod average length). The position of each node on the y-axis indicates its average length in that year, arrows point from the source species to the target species and the color gives the posterior mean interaction strength. For clarity, interactions with an absolute magnitude less than 0.05 are not shown.	38
3.4	Posterior estimates of the pairwise interaction coefficients in each year (the B_{ijt}). The black line indicates the posterior median, while the gray ribbon indicates the 90% posterior credible interval. The panels on the diagonal represent each species' effect on itself, which we model as a constant (the η_i), apart from the Gaussian process regression.	39
3.5	Stability quantities of the posterior mean \mathbf{B}_t . Larger values of $\max(\lambda)$, the magnitude of the dominant eigenvalue, correspond to longer return times following a perturbation. Larger values of reactivity indicate a tendency to initially amplify perturbations. . . .	40
4.1	Posterior predicted interaction surface between pollock prey and arrowtooth flounder predators. The red shading indicates the mean posterior interaction probability (ϕ) between every length of predator (x-axis) and prey (y-axis). The points indicate the observation of a prey item in the stomach of a predator, with the size of the point indicating y , the number of predator stomachs in which that prey was observed. A full plot of all predator and prey species is available in the appendix.	56
4.2	The observed counts of prey in predator stomachs (the y_{ij}) plotted against the mean posterior expected counts ($\phi_{ij}J_i$). The line indicates the 1:1 line.	56
4.3	Model fits to node length (the x_i) and species identity (the s_i). The top panel plots the observed length of each node against its mean posterior predicted length (i.e., μ_{z_i}). The line indicates the 1:1 line. The bottom panel plots the mean posterior probability of each node's species label (i.e., θ_{z_i, s_i}).	57
4.4	Posterior distribution of the number of trophic groups.	58
4.5	Group membership of every node in the food web, taken from the consensus partition (i.e., the posterior sample whose group assignments z produce the group adjacency matrix that is closest to the full posterior affinity matrix). The groups are ordered by their average size μ_k	59
4.6	Group-wise interaction probabilities (the ϕ_{ij}) corresponding to the consensus partition. The shading of each cell represents the probability that a prey item in that column appears in the stomach of a predator in that row. The rows for groups containing only prey nodes were omitted.	60
4.7	The dimension-reduced food web. Each node corresponds to a group in the consensus partition, with labels matching Figure 4.5. The position of each node on the y-axis corresponds to its average length (i.e., μ_k). The black arrows point from prey to predator, with darker arrows corresponding to larger interaction probabilities (given in Figure 4.6). Interactions with a strength less than 0.03 were omitted for clarity. The red arrows indicate groups that are connected by ontogenetic niche shifts in the four top predators and pollock (the ontogenetic niche shifts of the basal species were omitted for clarity).	61

5.1	Lagged fluctuations in growth and survival. The top panel shows the posterior mean growth (dashed line), and posterior mean survival (solid line) for three sizes of juvenile cod. Each trajectory has been centered and scaled to have a mean of zero and standard deviation of one. The bottom panel gives the 3 year running average bottom temperature anomaly.	87
5.2	Posterior predicted interaction surface between all pairs of prey and predators. The red shading indicates the mean posterior interaction probability (ϕ) between every length of predator (x-axis) and prey (y-axis). The points indicate observations of a prey item in the stomach of a predator.	90

Chapter 1

Introduction

Predator-prey interactions fundamentally take place at the level of the individual (Hartvig et al. 2011). Variation among individuals in their traits and states means that there can be substantial variability in individual resource use (Bolnick et al. 2003) and in the interactions in which individuals of the same species participate. This variation may be driven by individual differences in preference or foraging traits (e.g., in sea otters (Tinker et al. 2012)), or by complex life histories and individual ontogeny (Werner and Gilliam 1984). Such ontogenetic niche shifts, changes in an individual's resource use as it grows or ages, are widespread in nature, with particularly dramatic examples in amphibians, aquatic insects, and fish (Werner and Gilliam 1984). In fish communities in particular, life history and trophic ecology are both critically linked to size (Andersen et al. 2016). In these systems individual size can grow over several orders of magnitude (Hartvig et al. 2011). For large predator species, individuals thus traverse nearly the entire food web as they grow.

These tremendous changes in trophic position over an individual's life history mean that predator-prey interactions cannot be viewed as occurring among species with single, fixed trophic roles (Polis 1984). Instead, each species is a continuous size-spectrum of individuals, each of whom may occupy a different trophic position. This perspective allows us to recognize, for instance, that juveniles of a large-bodied predator species may occupy a similar trophic position as adults of a small-bodied prey species. Thus food web and predator-prey theory based on individual life history may differ from theory developed at the species-level (de Roos and Persson 2002). Size-spectrum (Hartvig et al. 2011) and physiologically structured (de Roos and Persson 2001) population models have been developed to explore the consequences of this disaggregation of predator-prey relationships. These frameworks capture ontogenetic structure by modeling the flow of individuals through time and along a size axis, accounting for changes in an individual's prey (which determine growth rate) and predators (which determine mortality) as it moves along that axis. Size-structured mod-

els thus provide a bridge between the individual and the population (Botsford 1981), and critically, between the individual and the community.

The large body of theory that has developed based on these frameworks highlights the unexpected indirect effects that can emerge in size-structured predator prey systems (de Roos and Persson 2002, van Kooten et al. 2005, van Leeuwen et al. 2008, 2013, 2014, Hartvig and Andersen 2013). These indirect effects emerge in large part from the ability of predators and prey to shape each other's growth environment and to create or relax growth bottlenecks at various points in their life history. Thus predators may release their favored sizes of prey from competition, thereby enhancing their growth and shifting the size structure of the prey population (de Roos and Persson 2002, van Leeuwen et al. 2008), or prey may compete for resources with, and impose a competitive bottleneck on, juveniles of their predator (Walters and Kitchell 2001).

This work has suggested that indirect effects may be particularly important in mediating system response to, and recovery from, fishing. In particular, resolving the full life history of the species in a community reveals that removal of large individuals can induce trophic cascades that ripple across both the system's mortality and growth regimes, causing alternating patterns of food limitation and competitive release (Andersen and Pedersen 2010). Moreover, the top-down control exerted by predators on the size-distribution of their prey can generate a catastrophic collapse of the predator as fishing mortality is increased (de Roos and Persson 2002), or prevent the recovery of a predator from low levels (van Kooten et al. 2005, van Leeuwen et al. 2008).

Despite the insights generated by this theoretical work, and the hypothesized importance of size-structured mechanisms in driving the dynamics of marine communities, the mechanistic complexity of size-structured models has made it difficult to make data-driven inference in real systems (Andersen et al. 2016, Spence et al. 2016). This difficulty has led both to limited opportunities to test and expand this theory for real systems, and a gap between theoretical ecology and its application in fisheries management (Collie et al. 2016). Addressing this disconnect, and learning from real systems, requires developing tools that allow us to confront these mechanistic theories with data. However, confronting mechanistic models with data is often challenging (Girolami 2008,

Wikle and Hooten 2010, Calderhead and Girolami 2011) and requires developing approaches that balance mechanistic fidelity with the statistical flexibility required to learn from data. Moreover, developing models that can be applied in fisheries management requires finding the ‘sweet spot’ that balances including additional ecosystem components with the added uncertainty those components may introduce (Collie et al. 2016).

In this dissertation, I seek this balance by recognizing that drawing complex mechanistic insights from noisy data often requires incorporating greater statistical flexibility in the process component of the model. Tailoring this flexibility, and aligning its application with the underlying biological motivation allows us to capture critical components of size-structured predator-prey relationships, while remaining tractable enough to fit to data. Each of the three chapters that follow deal with the role of size and ontogeny in determining the structure and dynamics of marine fish communities, but each chapter takes a different approach to navigating the above complexity-uncertainty trade-off. More specifically, in each chapter, I collapse some dimension of the full species-by-size interaction milieu (McGill et al. 2006) while retaining others to gain insight into two exploited marine ecosystems. Chapters 2 and 3 both focus on the dynamics of the Scotian Shelf community, where the cod fishery provides one of the classic examples of fisheries collapse. Chapter 4 focuses on the structure of the Gulf of Alaska ecosystem, which, together with the Bering Sea, supports the largest commercial fishery by volume in the United States (Gaichas et al. 2015).

Chapter 2 focuses on the dynamics of the Scotian Shelf cod population, and the processes that have prevented its recovery following its collapse and the closure of the fishery in 1993. In particular, I explore how the demographic landscape faced by individual cod changed from 1983 to 2003, trying to capture the feedbacks that may have been generated by its collapse and the subsequent trophic cascade (Frank et al. 2005). In this framework, by focusing on just the cod population, I subsume the full interaction milieu into its effect on cod length-specific growth and survival rates. This allows us to capture cod life-history and the dynamics of its length-distribution in detail, which in turn allows us to identify bottlenecks that may be preventing cod’s recovery from low

abundance. I then explore whether the identified demographic landscape is consistent with the hypotheses generated by the theory discussed above.

Chapter 3 provides greater community-context for the insights generated by Chapter 2. In particular, I expand the scope beyond just cod to include haddock, the other dominant large-bodied predator, the forage fish herring and sandlance, and their interactions. To accommodate this larger species diversity, I simplify our representation of the size-structure within each species. I model the dynamics of each species' total abundance as a function of interspecific interactions that depend on species average lengths and how they change through time (e.g., as large-bodied individuals are lost from harvesting). This approach allows us to take advantage of the theory and methods that have been developed for modeling community dynamics, while also capturing the role that changing length-distributions may play in governing the net effect of one species on another. Modeling the cod-forage fish interactions also allows us to further investigate the role that forage fish may play in preventing cod recovery, and to connect the demographic changes identified in Chapter 2 to the broader community. The multi-species model developed in Chapter 2 also enables us to connect changes in interaction structure (driven by changes in species length-distribution) to changes in system stability.

While Chapters 2 and 3 focus on the role of size-structure in driving population and community dynamics, Chapter 4 focuses on food web structure and identifying how species in a size-structured community partition ontogenetic niches. In this chapter, I handle the full variability of size-structured predator prey interactions by developing methods to describe the system with a lower-dimensional set of trophic groups containing individuals with similar interaction patterns. This allows me to describe the key features of an ontogenetically resolved food web without needing to *a priori* aggregate over either species or size. The resulting dimension-reduced description of the food web then highlights patterns of niche overlap in the community, and the different routes through which energy flows.

In summary, Chapter 2 collapses the community context surrounding Scotian Shelf cod while maintaining detailed demographic resolution within cod. Chapter 3 complements this work by of-

fering greater resolution on the community dynamics and interactions on the Scotian Shelf, while collapsing intraspecific structure to total abundance and average length. Together, these two chapters investigate changes to both the demographic and interaction landscape of Scotian Shelf cod and evaluate the predictions of theory about the recovery prospects of a large-bodied predator in a real system. Lastly, Chapter 4 develops a data-driven approach to reduce the dimension of an individual-level food web and describe the shared ontogenetic backbone of a marine community. Taken together, this research further advances the effort to better understand community ecology from an individual-level perspective (Bolnick et al. 2003), while recognizing that incorporating that perspective into models of real systems is likely to require careful choices about model structure and complexity.

Chapter 2

The changing demographic landscape of Scotian

Shelf cod

2.1 Introduction

Identifying the demographic factors contributing to or limiting population growth is critical for understanding the potential for depleted populations to recover (Caughley 1994, Benton and Grant 1999). Understanding the factors that may limit recovery is particularly important in fisheries ecology and management, where many collapsed fish stocks have remained at low abundance despite reductions in fishing pressure (Hutchings 2000, Neubauer et al. 2013). In fact, reduction of fishing broadly seems to be insufficient for recovery, suggesting that other processes or feedbacks may be responsible for limiting population growth (Hutchings 2001). In particular, a population's ability to recover following a collapse is likely to be mediated by the rest of the community and the cascade of feedbacks and responses generated by its decline.

In particular, the release of forage fish prey from top-down control can play a crucial role in controlling the growth and mortality environment experienced by large-bodied predators following collapse (Gårdmark et al. 2015). The feedbacks generated from this loss of top-down control can create emergent Allee effects and alternative stable states through either cultivation/depensation or overcompensation processes (Gårdmark et al. 2015). In the cultivation/depensation hypothesis, Walters and Kitchell (2001) suggest that juvenile predators and forage fish prey compete for similar zooplankton resources, and that forage fish may even prey on predator eggs and larvae. Thus, by cropping down the forage fish population, adult predators “cultivate” a favorable environment for their juveniles. The collapse of the predator population, however, releases forage fish from control, generating predator-prey role reversal and/or a competitive bottleneck for juveniles of the once-dominant predator (Walters and Kitchell 2001). The overcompensation hypotheses posits

that top-down control from an abundant predator releases the surviving individuals of the forage fish population from competition, enabling better growth conditions and higher recruitment, all of which serves to generate more or higher-quality prey for large predators (de Roos and Persson 2002, van Kooten et al. 2005, van Leeuwen et al. 2008). In this scenario, the loss of top-down control creates a competitive bottleneck in the forage fish population, leading to reduced reproduction and little suitable prey for large predators, despite the large total abundance of forage fish. These two processes – cultivation/depensation and overcompensation – either alone or in concert, may serve to create poor conditions for a collapsed predator and prevent population growth from low levels (Gårdmark et al. 2015).

These bottom-up, emergent Allee effects have been proposed as potential explanations for the slow recovery of the collapsed Scotian Shelf cod (*Gadus morhua*) stock, despite the closure of the fishery in 1993 (Bundy 2005). The collapse of the cod population in the early 1990s initiated an apparent trophic cascade (Frank et al. 2005) and a shift from a community dominated by large-bodied bottom fish to a community dominated by small pelagic forage fish and benthic invertebrates (Bundy 2005, Frank et al. 2005). Despite the closure of the cod fishery, this state has persisted, with only recent signs of recovery and emergence from a prolonged transient (Frank et al. 2011). The apparent release of forage fish from top-down control suggests a potential role for cultivation/depensation and overcompensation. However, several studies have suggested that the interaction between cod and forage fish has played a relatively small role in driving changes in community structure and suppressing cod (O’Boyle and Sinclair 2012, Swain and Mohn 2012, Sinclair et al. 2015). Instead, these studies suggest that cod recovery may be suppressed by predation mortality exerted by the rapidly growing grey seal (*Halichoerus grypus*) population on the Scotian Shelf (O’Boyle and Sinclair 2012). Such mortality on a population already at low abundance could also generate an emergent Allee effect and prevent recovery (Kuparinen and Hutchings 2014, Neuenhoff et al. 2018).

Evaluating the contribution of these bottom-up and top-down processes to the continued low abundance of Scotian Shelf cod requires a detailed understanding of how cod demographic pro-

cesses have changed following the collapse, and how those changes have influenced the potential for population growth. Many anomalies have been identified in cod population processes (e.g., high mortality of mature cod Sinclair et al. (2015)), but have not been demonstrated as a limiting factor for population growth, nor have the relative strengths of different limiting factors been compared. Moreover, many of the existing analyses of the Scotian Shelf cod population have been correlative, or have relied on models with restrictive assumptions (e.g., equilibrium) or coarse resolution of cod life history (e.g., juveniles and adults). Given the nature of the hypotheses for the slow recovery of cod, there is a need for more realistic, flexible models of cod population dynamics (Fu et al. 2001) that account for size-based demographic processes and the close relationship between mortality and growth in regulating population size (Werner and Gilliam 1984).

In this chapter, we developed a size-structured model of cod population dynamics to estimate fluctuations in cod growth and mortality processes across both time and length. We used these estimates to identify changes in the growth and mortality landscape of cod following its collapse and identify possible bottlenecks that may be responsible for limiting recovery. Specifically, we evaluated whether the estimated demographic changes are consistent with cultivation/depensation, overcompensation, and/or seal predation.

2.2 Methods

Modeling cod population dynamics involves uncertainty across multiple levels – the data level involving noisy survey observations, the process level capturing length-structured demographic processes, and the parameter level – thus, we embedded our model in a Bayesian hierarchical framework (Berliner 1996). This framework involves a joint likelihood that combines two sources of survey data, both linked to an underlying length-structured population model. This population model is governed by time- and length-varying growth and survival processes that we then used for long-term simulations and sensitivity analyses to parse the factors limiting cod recovery.

2.2.1 Data model

Growth and mortality processes are tightly linked drivers of population dynamics and size-structure (Werner and Gilliam 1984, Hartvig et al. 2011). In particular, growth has a direct effect on abundance by controlling how long an individual is exposed to different mortality pressures at different lengths (Parma and Deriso 1990, Byström et al. 1998). Moreover, mortality can have a large effect on how the length distribution of a given cohort evolves (e.g., if the largest individuals of a cohort face higher mortality, Parma and Deriso 1990, Gudmundsson 2005). To simultaneously estimate both length-specific growth and mortality, we made use of two data sets, both collected by the Department of Fisheries and Oceans Canada from fisheries-independent bottom-trawl surveys of the Eastern Scotian Shelf (region 4VsW) in July/August each year from 1983 to 2003. The first data set consists of estimates of the mean length of cod as a function of age, providing information on how the average length of a cohort changes as it ages (due to both growth and length-specific mortality). The second data set consists of average catch per tow (i.e., bottom trawl sample), binned in 48 3cm length bins ranging from 4 to 142cm, providing estimates of how the cod length distribution (i.e., cod abundance as a function of length) changes through time (due to both growth and mortality). Together, these two data sets capture two different dimensions of cod population structure (the age-length dimension and the abundance-length dimension) and allowed us to simultaneously estimate the rates at which individuals move along the length axis and the rates at which they are lost from the population.

Let z_{at} be the average length of cod at age a and time t , and y_{it} be the average number of fish caught per tow in length bin i , bounded by (l_i, l_{i+1}) , in year t . We modeled the length-at-age data with a log-normal likelihood:

$$z_{at} \sim \text{LogNormal}(\mu_{at}, \sigma_z^2)$$

where

$$\mu_{at} = \log(\bar{x}_{at}) - \sigma_z^2/2$$

such that $E[z_{at}] = \bar{x}_{at}$, the latent true average length of age a fish in year t (potentially averaging over multiple cohorts within that age class). Because the catch-at-length data are an average abundance index, the y_{it} are continuous, with zeros reported for length-bins in which no fish were observed. To match this support, we specified a truncated normal likelihood where the standard deviation scales linearly with the mean (enabling similar flexibility to a log-normal distribution, but with mass at zero):

$$y_{it} \sim \text{TN}(q_i \lambda_{it}, (\sigma_y q_i \lambda_{it})^2)$$

where λ_{it} is the latent abundance in length bin i in year t , σ_y scales the standard deviation relative to the mean, and q_i is the catchability of fish in length bin i . To account for the fact that small fish are less available to the survey gear, we modeled catchability as a logistic function of length (Harley et al. 2001):

$$q_i = q_{max} \frac{\exp(b_0 + b_1 l_i)}{1 + \exp(b_0 + b_1 l_i)}$$

where q_{max} is the maximum catchability, and b_0 and b_1 control the shape of the logistic function.

We obtained the true abundance in length bin i , λ_{it} by integrating over the latent continuous-length abundance spectrum, $\lambda(l, t)$ at time t :

$$\lambda_{it} = \int_{l_i}^{l_{i+1}} \lambda(l, t) dl.$$

2.2.2 Chew-chew train process model

Size-structured population models (e.g., Hartvig et al. 2011) link the size spectrum to growth and mortality through the McKendrick-von Foerster partial differential equation:

$$\frac{\partial \lambda(l, t)}{\partial t} = -\frac{\partial}{\partial l} (g(l, t) \lambda(l, t)) - \mu(l, t) \lambda(l, t)$$

where $g(l, t)$ and $\mu(l, t)$ are the growth and mortality rates of length l fish at time t .

Rather than solve this PDE directly, we adopted a discrete-time version of the ‘‘escalator boxcar train’’ (de Roos et al. 1992) method in which we approximated the above length spectrum by

breaking the population into discrete cohorts characterized by their abundance and average length. We then smoothed these cohorts into the continuous length spectrum with a process convolution (Higdon 2002, Hefley et al. 2017):

$$\lambda_t(l) = \sum_j n_{jt} K(x_{jt} - l)$$

where $K(\cdot)$ is a squared exponential kernel with length scale σ_{Kl} , and n_{jt} and x_{jt} are the abundance and average length of fish of cohort j at time t . Smoothing the discrete cohorts into a continuous length spectrum allowed us to convert the cohort abundances into the expected abundances in the length bins of the data.

Changes in the length spectrum through time are induced by changes in the abundance and average length of the underlying cohorts due to growth and mortality processes. We modeled this cohort evolution as:

$$\begin{aligned} n_{j+1,t+1} &= n_{jt} \phi(x_{jt}, t) \\ x_{j+1,t+1} &= x_{jt} + (x_\infty - x_{jt}) g(x_{jt}, t), \end{aligned}$$

where $\phi(x, t)$ is the survival of length x fish from t to $t + \Delta t$, x_∞ is the asymptotic length, and $g(x, t)$ is the proportion of the remaining available length grown by a length x fish from t to $t + \Delta t$. Bounding $\phi(x, t)$ and $g(x, t)$ between zero and one ensures that the abundance of a cohort declines as it ages, while the average length of a cohort increases and approaches (but does not exceed) its asymptotic length. We modeled these survival and growth processes using a process convolution framework (Higdon 2002), in which continuous surfaces over time and length were obtained by smoothing i.i.d normal random variables positioned on a fixed grid over length and time:

$$\begin{aligned} \text{logit}(\phi(x, t)) &= \phi_0 + \sum_k \xi_k K_x(x - u_k) K_t(t - \tau_k) \\ \text{logit}(g(x, t)) &= g_0 + \sum_k \epsilon_k K_x(x - u_k) K_t(t - \tau_k) \\ \xi_k &\sim \text{Normal}(0, \sigma_\xi^2) \\ \epsilon_k &\sim \text{Normal}(0, \sigma_\epsilon^2) \end{aligned}$$

where ϕ_0 and g_0 control the overall mean survival and growth, respectively, ξ_k and ϵ_k are the random variables associated with the k th grid point, located at length u_k and time τ_k , and $K_x(\cdot)$ and $K_t(\cdot)$ and are independent squared exponential smoothing kernels parameterized by characteristic length scales σ_{K_x} and σ_{K_t} , respectively. The process convolution framework generates smooth survival and growth surfaces over length and time that characterize the changes in the demographic landscape of cod. The smoothness of these surfaces, which captures the assumption that fish of a similar length should experience similar growth and survival conditions, also allowed us to pool information across time and length, helping alleviate issues with data sparsity or quality.

2.2.3 Parameterization and priors

The boundary conditions were defined by the initial conditions (\mathbf{n}_0 and \mathbf{x}_0) and the abundance and length of the new cohort that recruits to the population at every time step (\mathbf{n}_1 and \mathbf{x}_1). To constrain the dimension of the initial conditions, we assumed that the sizes of the initial cohorts, x_{j0} , follow the commonly used von Bertalanffy growth curve:

$$x_{j0} = x_\infty - (x_\infty - x_0) \exp(-\kappa j \Delta t)$$

where κ is the von Bertalanffy growth constant and x_0 is the length at age 0, and $j \Delta t$ gives the age of cohort j . We modeled the abundances of the initial cohorts with a flexible process convolution over the length axis:

$$\log(n_{i0}) = \sum_k \eta_k K_x(x_{i0} - u_k)$$

$$\eta_k \sim \text{Normal}(0, \sigma_\eta^2).$$

We modeled the abundance of new recruits using a Ricker stock-recruitment relationship, as in Swain and Mohn (2012):

$$n_{1t} = \nu S_t \exp(-\delta S_t)$$

where ν and δ control the linear and density dependent components, respectively, and S_t is spawning stock biomass in year t . This was computed as:

$$S_t = \sum_j \left[1 + \left(\frac{x_{jt}}{x_*} \right)^{-10} \right]^{-1} n_{jt} \alpha x_{jt}^\beta$$

where the first term is a function that transitions smoothly from 0 to 1 around the length-at-maturity, x_* , and α and β convert length (cm) to weight (g). We held the size at recruitment constant, such that $x_{1t} = x_{11}$ for all t .

Lastly, we placed priors on the boundary condition parameters, κ , x_0 , ν , and δ , the mean survival, ϕ_0 , and growth, g_0 , and the measurement dispersion parameters, σ_y and σ_z . See the appendix for full model specification and priors. The remaining constants, including cod size-at-maturity and asymptotic length, and the process convolution grid and standard deviations were fixed at values given in Table 1.

Table 2.1: Model parameters, their description, and their values.

Parameter	Description	Value	Citation
x_*	Length at maturity	40 cm	(Hall and Collie 2006)
x_∞	Maximum length	148 cm	(Hall and Collie 2006)
q_{max}	Maximum catchability	0.95	(Harley et al. 2001)
b_0	Catchability coefficient	-5.0	(Harley et al. 2001)
b_1	Catchability coefficient	0.14	(Harley et al. 2001)
α	Length-weight prefactor	0.007	
β	Length-weight exponent	3	
σ_{K_l}	Length scale of K_l	3.0 cm	
σ_{K_x}	Length scale of K_x	10 cm	

Parameter	Description	Value	Citation
σ_{Kt}	Length scale of K_t	3.0 years	
u	Grid locations on length axis for ϵ and ξ	0, 10, \dots , 140	
τ	Grid locations on time axis for ϵ and ξ	1980, 1983, \dots , 2004	

2.2.4 Implementation and sampling

We implemented our discrete-time escalator boxcar train in the Julia language (Bezanson et al. 2017). We used a step size (Δt) of six months, providing two cohorts a year to roughly correspond with the spring and fall spawning components of the cod stock (Frank et al. 1994). We fixed the maximum age at 15 years, producing a population with 30 cohorts (i.e., $j = 1, \dots, 30$), with two cohorts belonging to every integer age class and contributing to every \bar{x}_{at} . Samples from the posterior distribution of all parameters were obtained using a Hamiltonian Monte Carlo algorithm, using the DynamicHMC package (Papp and Piibeleht 2019). Multiple chains were run for 1000 iterations after warm-up and burn-in and checked for convergence.

2.2.5 Evaluating long-term population growth and sensitivity

To parse the consequences of fluctuations in growth and survival, for each year, t , we froze the growth and survival regime for that year (i.e., we collapsed growth and survival to a fixed function of length, such that $g(x) = g(x, t)$, and $\phi(x) = \phi(x, t)$) and projected the population 20 years forward from that time. We used the predicted spawning stock biomass 20 years ahead to evaluate whether a given set of demographic conditions lead to population growth (i.e., favorable conditions) or decline (i.e., poor conditions). We also computed the sensitivity of the spawning stock biomass at the end of each of those 20 year simulations to changes in each of the process-convolution parameters (the ϵ_k and ξ_k) that governed the growth and survival regimes used in the simulation. Let Q be the spawning stock biomass at the end of 20 years, and let θ_t be the process

convolution parameters from a given sample from the posterior, fixed at their values in year t . Then we computed the sensitivities as the partial derivative $\partial Q(\boldsymbol{\theta}_t)/\partial \boldsymbol{\theta}_t$, using the ForwardDiff library in Julia (Revels et al. 2016). These estimated sensitivities provide information on how small changes in growth and survival at a particular size (i.e., a particular u_k) are predicted to affect the long term spawning stock biomass.

Our yearly estimates of growth and survival taken together give a range of biologically realistic growth and survival rates. To further evaluate the relative contribution of different growth and survival regimes to cod population growth, we performed an additional set of simulations in which we projected the dynamics of the cod population forward from 2003 using every combination of growth and survival regime estimated over the course of the time series. More specifically, we simulated 20 years of dynamics forward from 2003 holding the survival regime as a function of length fixed at its values in year t , (i.e., $\phi(x) = \phi(x, t)$) and holding the growth regime fixed at its values in year t' (i.e., $g(x) = g(x, t')$), for all pairs of t and t' . This allowed us to separate the effects of the paired growth and survival regimes explored in the simulations and better isolate the effects of variation in both growth and survival.

2.3 Results

The model successfully captured the overall decrease in the slope of the length-at-age curves over time (Fig. 2.1). The model also captured the the long-term decline in abundance in the observed catch-at-length data (Fig. 2.2). However, the agreement between the observed catch-at-length distributions and the model predictions varied by year. In particular, due to the smoothness constraints of the process-convolution, we were unable to characterize abrupt changes in the size distribution (e.g., the sudden drop in abundance from 1985 to 1986).

Growth and survival conditions fluctuated through time for all sizes of cod (Figure 2.3). For juvenile cod (less than 40cm), growth conditions declined throughout the 1980s, bottoming out around 1990 before recovering slightly in the late 1990s and declining again (Figure 2.3). At the same time, juvenile cod experienced favorable survival conditions in the late 1980s that deterio-

rated around the time of the fishery closure and again rebounded slightly in the late 1990s before declining. The growth conditions for large cod (greater than 50cm) followed roughly the opposite trend as the juveniles. The growth rates of large cod increased from 1983 through the early 1990s, then broadly declined thereafter (Figure 2.3). While growth rates improved throughout the 1980s, survival of large cod declined, reaching a minimum in the early 1990s and recovering slightly following the fishery closure (Figure 2.3). Due to how infrequently they were observed in either data set, the estimates of growth and survival of the largest cod (greater than 80 cm) were not well informed by the data.

Simulating the long-term dynamics generated by the demographic conditions in each year indicates that there were large fluctuations in the potential for cod population growth and maintenance (Figure 2.4). In particular, our simulations suggest that the demographic conditions around the time of the fishery closure were very poor, and were predicted to lead to local extinction of the cod population in the long term (Figure 2.4). By 1998, conditions had (briefly) improved, with our simulations predicting long-term maintenance and slight recovery (Figure 2.4). These conditions were short-lived, however, and our simulations predicted that the conditions in 2003 would again lead to local extinction if held constant.

To better separate the contributions of the growth and survival regimes to the potential for cod recovery from its 2003 levels, we performed further simulations in which we varied the growth and mortality separately, exploring all possible combinations of estimated annual regimes. These simulations suggest that the long-term dynamics respond much more strongly to the historical range of mortality conditions than to growth conditions (Figure 2.5). In particular, we identified three survival regimes – 1983-1984 (potentially an artifact of the initial conditions), 1992-1995, and 2002-2003 – in which cod were predicted to go locally extinct, regardless of the growth regime. Variation in the growth regime only had an effect on the long-term spawning stock biomass when paired with survival regimes that supported long-term persistence. Further, although poor growth conditions (as in the early 2000s, for example) could reduce the long-term spawning stock biomass

relative to better regimes, there were no growth regimes that were predicted to lead to local extinction.

We further found that the long-term spawning stock biomass, simulated ahead from 2003, was most sensitive to the process convolution parameters corresponding to the growth of 40cm cod and the survival of 30 cm cod. High sensitivity to these parameters was remarkably constant over all of the demographic regimes (results not shown).

2.4 Discussion

There have been a number of studies of Scotian Shelf cod that estimate temporally-varying age or stage (e.g., juvenile and adult) specific mortality, but relatively few have coupled those mortality estimates with growth to account for the joint effect of growth and survival on population dynamics. The model that we developed here allowed us to estimate fluctuations in cod growth and survival conditions across both length and time and to evaluate the consequences of those fluctuations for cod productivity. Consistent with the collapse of the cod population and the subsequent apparent reorganization of the Scotian Shelf community (Bundy 2005, Frank et al. 2005), we observed substantial variation in the demographic landscape of the cod population over the 20 years studied (Figure 2.3). Moreover, we found that demographic variation generated considerable variation in the long-term productivity potential for cod, with several periods of very poor demographic conditions that were predicted to lead to population decline.

In particular, our simulations of long-term cod population dynamics suggest that the growth and survival regimes present in 2003, if held constant, would likely lead to local extinction of cod (Figure 2.4). By repeating this simulation with different combinations of historical growth and survival regimes, we found that the poor survival regime present in 2003 was the primary driver of the predicted long-term decline. Thus, consistent with other analyses of Scotian Shelf cod, we found that poor survival conditions were ultimately the limiting factor in cod recovery, as of 2003 (Fu et al. 2001, Bundy and Fanning 2005, Swain and Mohn 2012, Sinclair et al. 2015). However, our simulations also revealed that survival conditions were not consistently poor following the

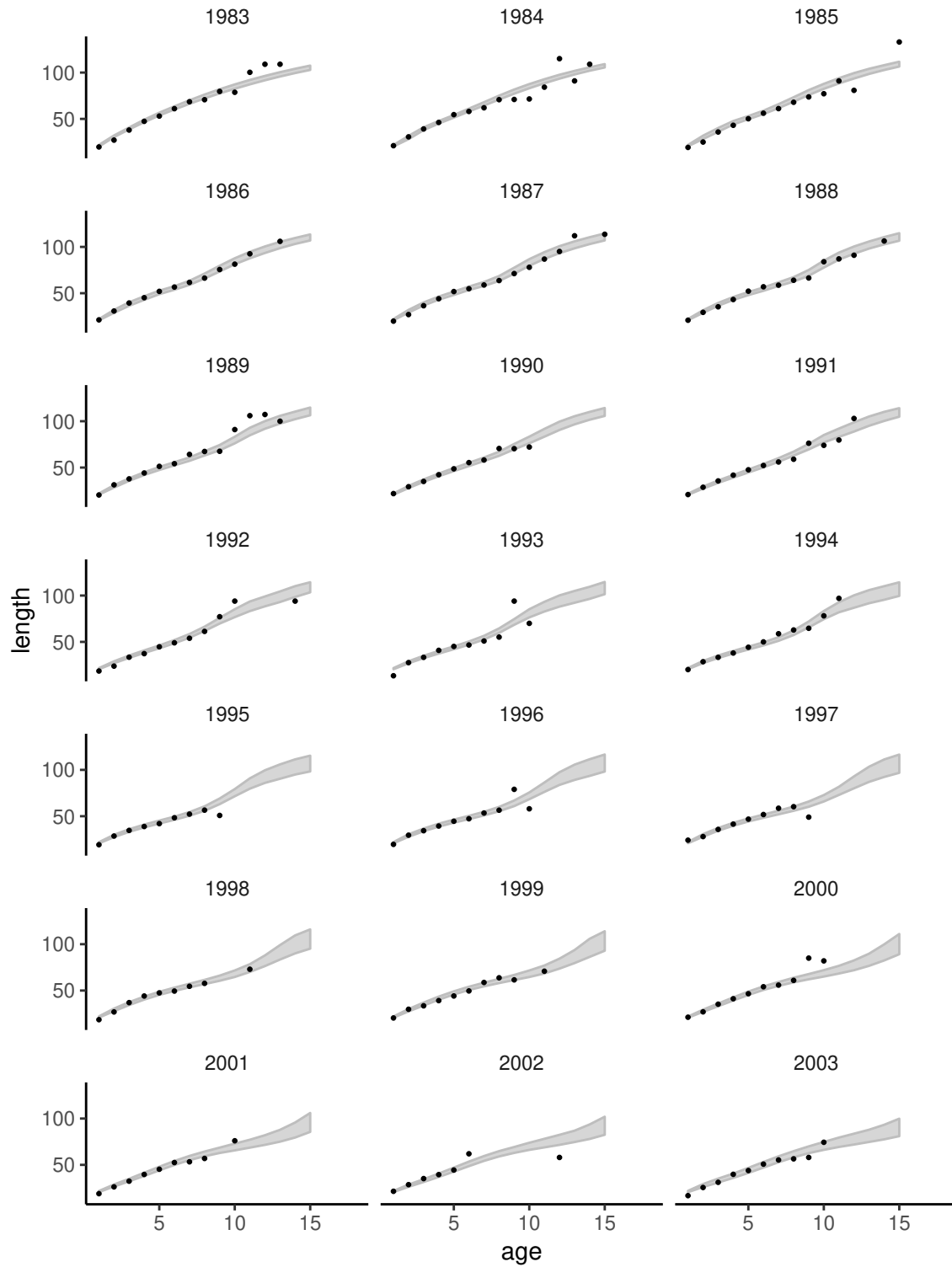


Figure 2.1: Length-at-age data and model predictions. The points represent the observed average length as a function of age, and the gray ribbon represents the posterior 95% credible interval of the w_{at} .

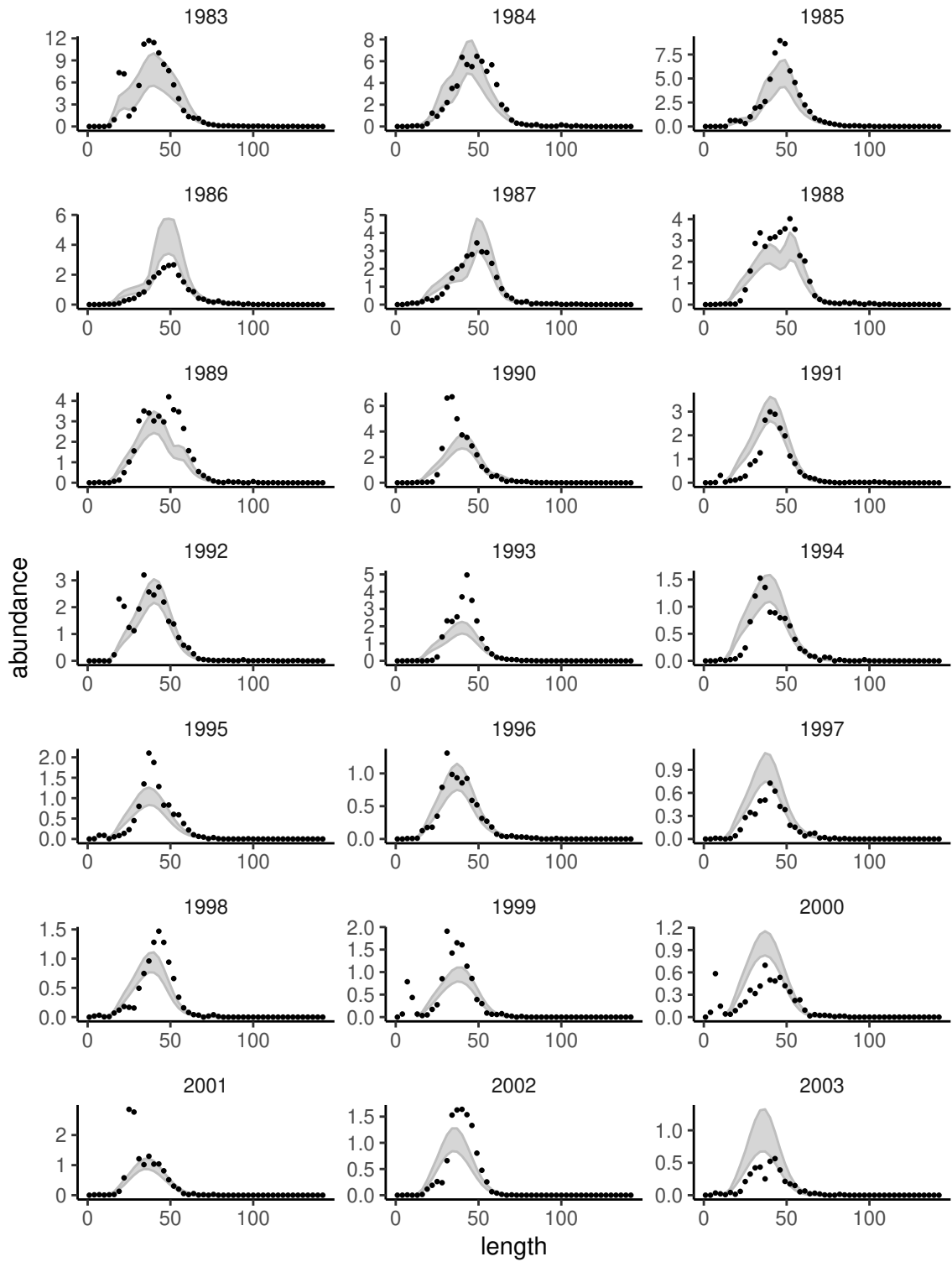


Figure 2.2: Catch-at-length data and model predictions. The points represent the observed average abundance per trawlable unit in 3cm length bins, and the gray ribbon represents the posterior 95% credible interval of the catchability-scaled λ_{it} .

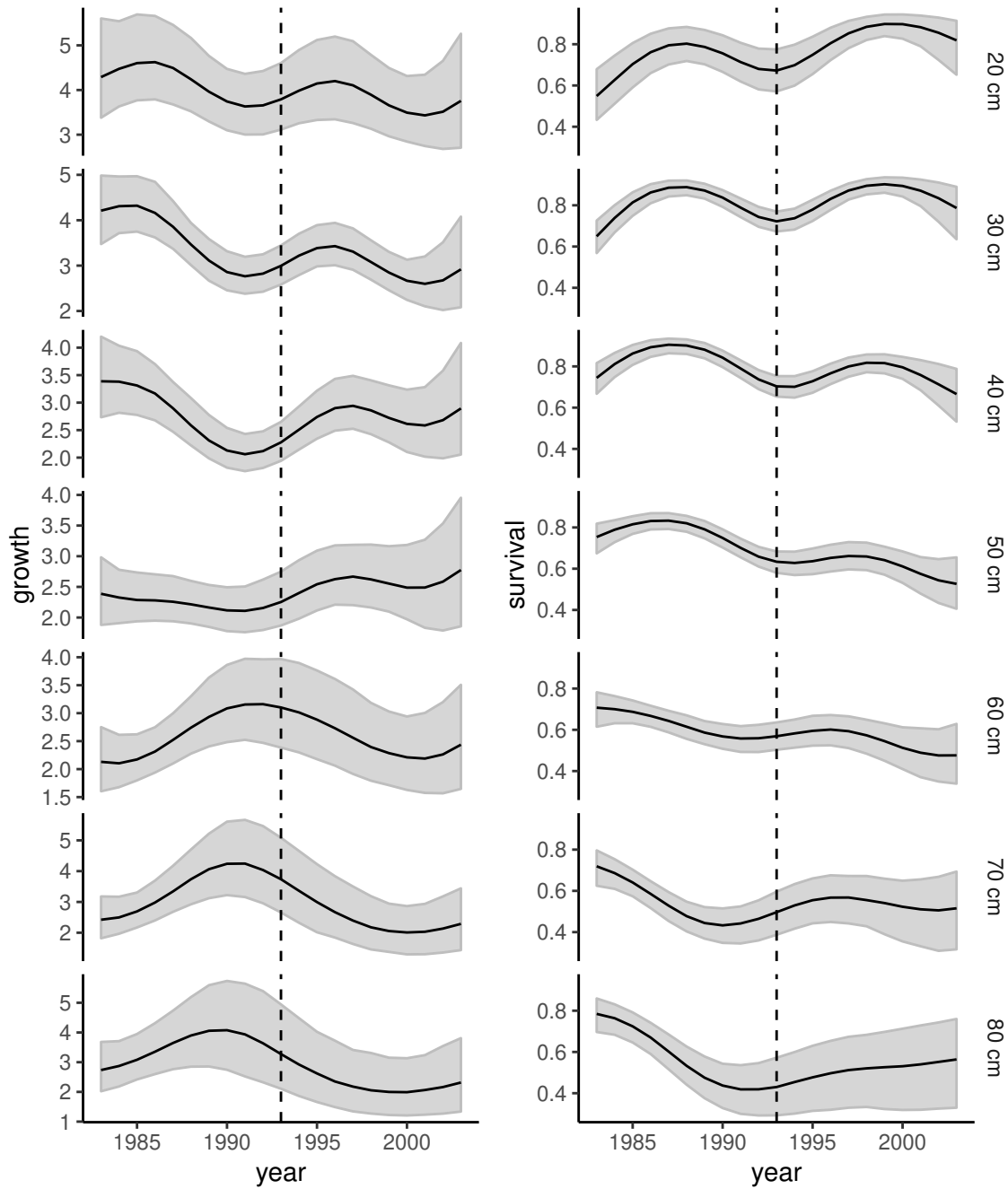


Figure 2.3: Estimated growth and survival trajectories for different sizes of cod through time. The panels on the left show estimated 6 month growth increments. The panels on the right show the estimated 6 month survival probabilities. The black line indicates the posterior median, while the gray ribbon represents the posterior 95% credible interval. The dashed line indicates 1993, the year the cod fishery was closed.

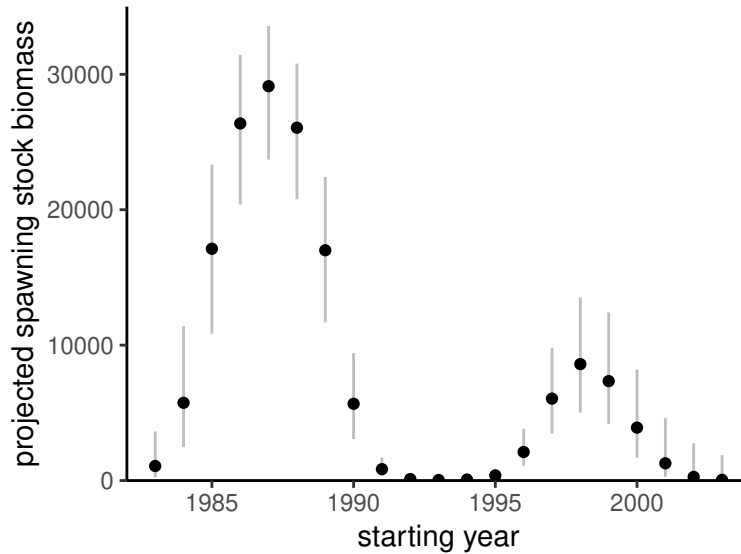


Figure 2.4: Projected spawning stock biomass 20 years ahead as a function of the initial year of the simulation, where growth and survival regimes were held constant at that year’s values. The black points indicate the posterior median, while the gray lines indicate the 95% credible interval.

collapse. Instead, we found that favorable survival conditions emerged in 1998 and 1999, most noticeably for 20 to 40 cm cod (Figure 2.3), and that these conditions would have facilitated a modest recovery had they remained in place (Figure 2.4, Figure 2.5). Several other studies also estimated a brief increase in cod survival around 1998 (O’Boyle and Sinclair 2012, Swain and Mohn 2012), but none actually linked that increase to a potential window for recovery.

The identification of this post-collapse fluctuation in survival regime suggests a possible diagnostic with which to evaluate hypotheses for the drivers of low survival in 2003. Predation mortality from seals, for example, appears to be inconsistent with this fluctuation. Though O’Boyle and Sinclair (2012) found that predation by seals could account for a large proportion of cod natural mortality throughout the 1990s, seal populations have been growing steadily for decades. A corresponding steady increase in predation pressure would thus not be consistent with the cod survival trends estimated here. Thus a more convincing link between cod survival and seal predation may require additional mechanisms (e.g., prey switching by seals) that generate the observed relaxation in mortality following collapse.

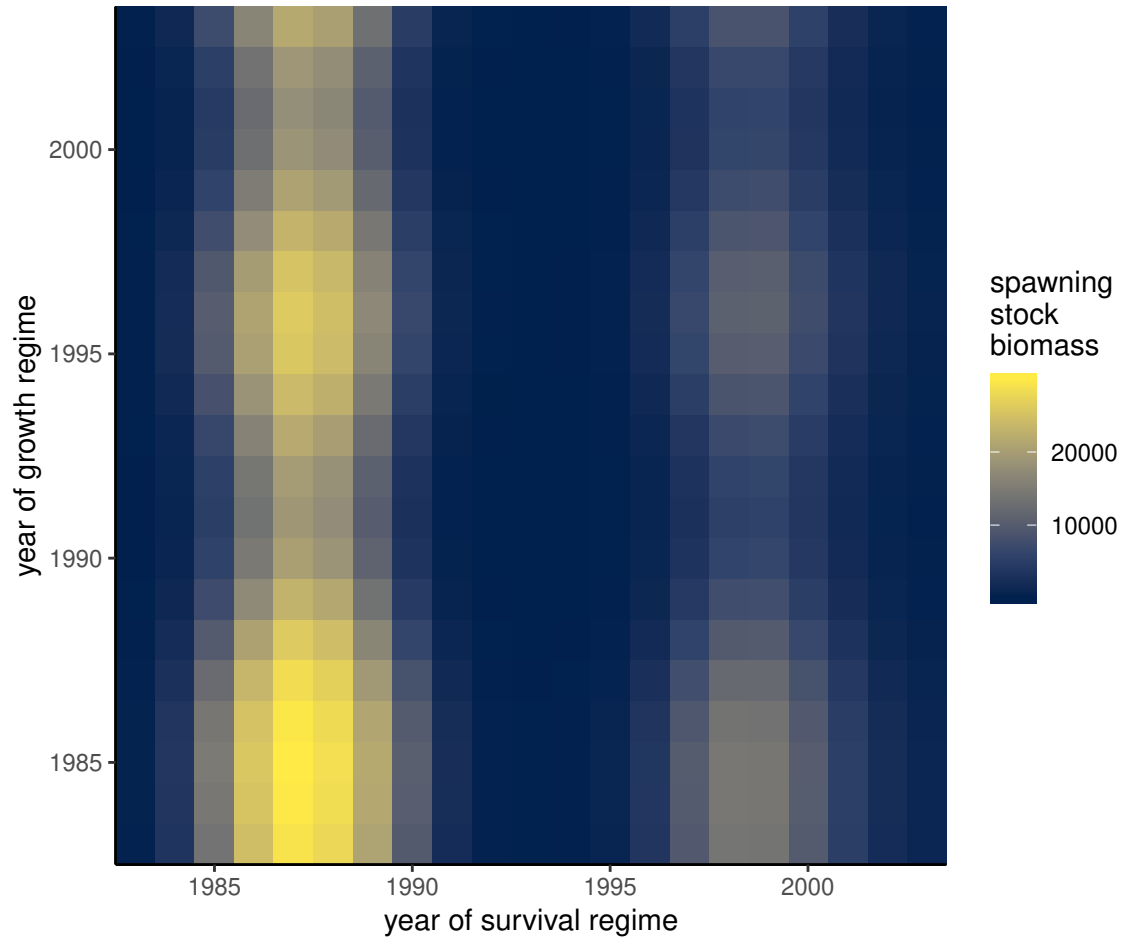


Figure 2.5: Heatmap of long-term spawning stock biomass predicted by simulating the population ahead 20 years from 2003, given growth and survival regimes fixed at their values in the given years. The dark blue regions correspond to demographic regimes predicted to lead to local extinction. The vertical banding of these regions indicates survival regimes for which no observed growth regime could prevent the predicted local extinction.

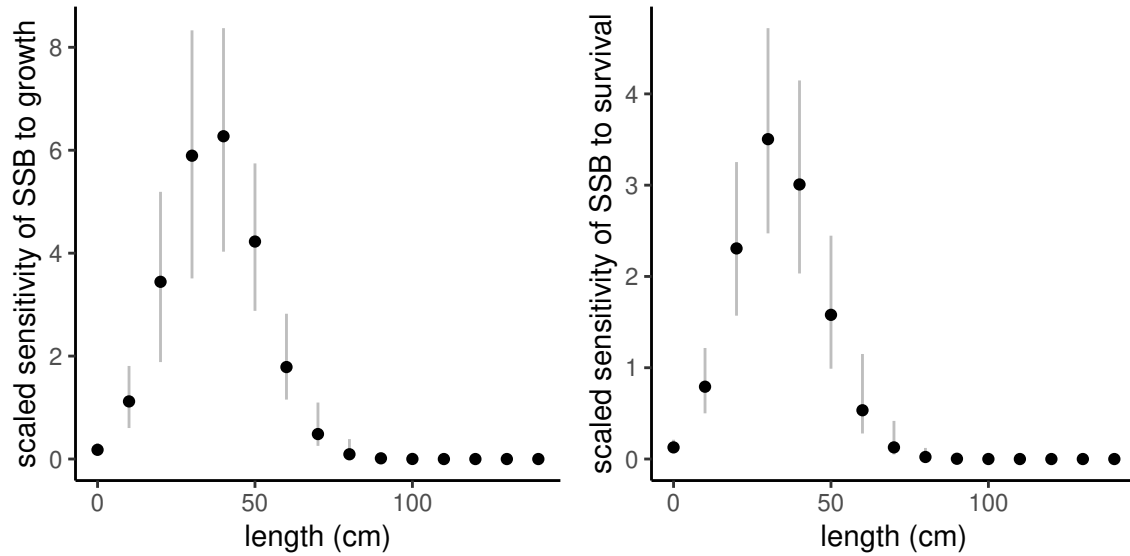


Figure 2.6: The scaled sensitivity of the projected spawning stock biomass 20 years ahead from 2003 to the growth (left) and survival (right) process convolution parameters located at the given size (i.e., $\partial\text{SSB}_{2023}/\partial\epsilon_k$, scaled by SSB_{2023} , where ϵ_k is located at length u_k). The points give the posterior median, while the lines give the posterior 95% credible intervals.

Growth processes, as mediated by the forage fish complex, provide an alternative hypothesis for the lack of cod recovery. Although growth does not appear to be limiting by itself, fluctuations in the growth regime may nonetheless reveal processes contributing to the survival bottleneck. Our estimates of the growth rates across length and time reveal a substantial decline in the growth conditions of large (60 - 80cm) cod throughout the 1990s, despite the large abundance of forage fish prey in the late 1990s. This disconnect between the growth conditions of large, piscivorous cod and the abundance of their forage fish prey supports the hypothesis that after release from top-down control, increased competition in the forage fish complex may be limiting their growth and their availability or benefit to cod (Gårdmark et al. 2015). Declines in forage fish condition beginning in the early 1990s provide support for the hypothesis that forage fish growth has been reduced in the face of intense competition (Frank et al. 2011). As such, though abundant, the forage fish prey available to large cod may be of such poor condition that they represent ‘junk food,’ on which large cod may not be able to persist (Gårdmark et al. 2015). This is consistent with the predictions of ‘overcompensatory’ dynamics in forage fish, and the resulting feedbacks

between predation pressure and the growth environments of both predators and prey (de Roos and Persson 2002, van Kooten et al. 2005, van Leeuwen et al. 2008).

At the same time, we found that growth conditions of juvenile cod were also relatively poor in the late 1990s, consistent with the timing of the forage fish boom. Bundy and Fanning (2005) identified a large overlap in the diet of small cod and forage fish, and predicted intense competition between the abundant forage fish and juvenile cod in the post-collapse period. Our estimates of depressed growth in juvenile cod suggest the presence of a competition-induced growth bottleneck and provide empirical support for the cultivation-dependence hypothesis (Walters and Kitchell 2001).

The decline in the growth conditions of cod in the late 1990s and early 2000s – coincident with the beginning of steady, high abundance of forage fish (Frank et al. 2011) – suggests that forage fish may play a key role in regulating the growth environment of cod in the post-collapse period. However, as our simulation experiments have shown, poor growth conditions alone are not sufficient to suppress cod recovery (Figure 2.5). Thus, for growth to limit the population dynamics of cod, it must have carry-over effects on survival and reproduction. Bundy and Fanning (2005) hypothesized that the poor growth of cod juveniles may lead to poor condition and increased mortality later in life. Further, Dutil and Lambert (2000) identified a link between poor condition, starvation mortality, and reduced cod productivity in the Gulf of St. Lawrence in the early 1990s.

Moreover, this possible link between poor growth and poor survival appears in the long-term oscillations that we estimate in the growth and survival of juvenile cod. Specifically, we identify poor survival conditions in the early 1980s and early 1990s, as well as in the early 2000s. Though the estimated conditions in the early 1980s are likely closely tied to the initial conditions, the declines in survival in the early 1990s and 2000s lag roughly two years behind declines in the growth regime (Figure 5.1). Though this trend should be interpreted with some caution, it is nevertheless consistent with the prediction that starvation mortality should lag behind poor growth conditions, as individuals are able to persist temporarily in the absence of resources by burning their energy reserves (Goulden and Hornig 1980).

While juvenile survival appears to be driven by growth, juvenile growth appears to be driven by changes in temperature, with better growth conditions corresponding to warmer temperatures in the early 1980s and 1990s and poor growth conditions corresponding to colder temperatures in the late 1980s (Figure 5.1). This points to a potential role for long-term climate forcing of juvenile growth rate (Swain et al. 2003), and a lagged carry-over effect on juvenile survival. The temperature-growth-survival sequence of forcing relationships also suggests an explanation for the late 1990s recovery window and the delayed onset of the poor survival regime in the early 2000s. Specifically, warm temperatures in the mid-1990s may have driven the initial improvement in growth and survival conditions following the collapse, before forage-fish induced food limitation took over as the primary driver of growth conditions. Though these patterns are compelling, the relationships between temperature forcing, growth, and mortality need to be further explored, potentially with a more detailed energetic model that explicitly accounts for energy reserves and the starvation mortality induced when they run out (e.g., de Roos and Persson 2001).

Simulating from their historical pattern of variability suggests broadly that poor survival regimes, potentially linked to poor growth regimes, are to blame for limiting cod population growth. Sensitivity analysis allows us to further diagnose at which sizes changes to the growth and survival regimes are likely to have the largest impact. These analyses suggest that increases in the survival of 30cm cod and the growth of 40cm cod are likely to make the largest impact on future biomass of the cod stock. The sensitivity of the long-term biomass to these parameters is relatively constant across different growth and mortality regimes, regardless of whether or not those regimes support long-term population growth. Though capturing the potentially disproportionate (relative to body mass) contribution of large individuals to recruitment (Barneche et al. 2018) could shift this sensitivity toward larger individuals, these results nevertheless highlight the importance of pre-breeding individuals (Reid et al. 2004), and the need to simply transition more fish across the maturity threshold (40 cm) and into the spawning stock.

2.4.1 Feedbacks

The presence of long-term oscillatory patterns in demographic conditions begs the question of whether the latest, unfavorable regime is permanent, or whether it too is the result of temporary fluctuations. The theory and modeling work behind the overcompensation (van Leeuwen et al. 2008), cultivation-dependence (Walters and Kitchell 2001), and seal-predation (Kuparinen and Hutchings 2014) hypotheses suggests that these mechanisms induce Allee effects and alternative stable states from which cod cannot recover. On the other hand, Frank et al. (2011) suggested that the prolonged period of low abundance is a long transient and that competition within the forage complex will damp out their oscillations in the long run and allow cod recovery. Our model is unable to distinguish between these hypotheses. However, we do predict that the demographic conditions faced by cod in 2003 would lead to local extinction. The continued persistence of cod on the Scotian Shelf suggests that more recent changes in the demographic conditions faced by cod (e.g., driven by the environment or feedbacks within the forage fish complex) may have averted that fate.

The long-term simulations that we carried out here assumed a fixed growth and survival landscape and thus did not account for the potential for these long-term changes or feedbacks. Better differentiating between a long transient and an alternative stable state driven by overcompensation or cultivation-dependence would require also understanding the growth environment of the forage fish complex, and the ability of cod to shape that growth environment prior to its collapse (Gårdmark et al. 2015). As such, future work should focus on closing this feedback loop by explicitly including forage fish, their interactions with cod, and their effects on a shared resource in the modeling framework (e.g., using the framework of Hartvig and Andersen 2013).

Further, we did not include density-dependent feedbacks on the growth and survival processes in the model. Instead, density dependence was captured through a Ricker stock-recruitment relationship (Swain and Mohn 2012). This prevents run-away population growth in our long-term simulations, but does not capture how resource depletion or cannibalism may induce density-dependent bottlenecks at other stages of life history (Andersen et al. 2016). Incorporating these

more flexible, mechanistic sources of density dependence into the modeling framework (e.g., by explicitly modeling a resource) may provide additional insights about bottlenecks that might emerge in our long-term simulations. However, we do not expect that the emergence of these bottlenecks would qualitatively change our predictions of which historical demographic conditions facilitate population growth and which do not.

2.4.2 Conclusions

To summarize, we found that cod recovery from its state in 2003 was limited by poor survival conditions. However, those survival conditions only emerged after 1998, prior to which conditions were briefly favorable for recovery. We argue that these fluctuations in survival may be driven by degradation of the growth environment resulting from both overcompensation and cultivation-dependence processes in the forage-fish complex. More broadly, for juvenile cod, temperature-driven fluctuations in growth rate may be responsible for long-term fluctuations in survival. Lastly, we predict that improving the growth and survival conditions of sub-adult (i.e., 30 - 40 cm) cod will have the largest effect on the population's long-term growth prospects. In size-structured populations like the Scotian Shelf cod, population growth emerges from the joint effects of growth, survival, and reproduction and their (co-) variation across cod life history. By accounting for these joint effects and their variation through time, while also remaining flexible enough to fit to and learn from survey data, the chew chew train was able to offer a more detailed and nuanced picture of the drivers of cod population dynamics and the potential for recovery.

Chapter 3

The changing interaction landscape of the Scotian Shelf fish community

3.1 Introduction

Community stability is a function of both species diversity and interaction structure (May 1972, Ives et al. 2003). In many communities, ontogenetic niche shifts within species (e.g., changes in habitat or resource use with an individual's size or age) create rich and complex interaction patterns among species (Werner and Gilliam 1984). The presence of these ontogenetic niche shifts means that different sized individuals of the same species occupy different functional roles within the community (Werner and Gilliam 1984, Garrison and Link 2000). As a result, changes in a species' size- or age-distribution, and the loss or reduction of particular components of that distribution, can alter the net sign and strength of its interactions with the rest of the community (Miller and Rudolf 2011, Rudolf and Rasmussen 2013), with corresponding consequences for community dynamics and stability.

The potential for ontogeny to induce changes in a system's interaction structure and stability is particularly important in marine fish communities, where ontogenetic niche shifts are common, as are size-selective fisheries that target particular functional components of a population. In fact, both theoretical (Andersen and Pedersen 2010) and empirical studies (Shackell et al. 2010) have demonstrated that selective fishing can induce trophic cascades through the removal of large-bodied individuals, even without the complete removal of any predators. Moreover, in size-structured marine communities, the net effect of one species on another emerges from a mix of both competitive and predator-prey relationships spread out over each species' life history (Hartvig and Andersen 2013). Thus, changes to species size distributions may induce changes in the relative strength of these mixed relationships. Addressing the growing need to incorporate species interactions into

fisheries management (Travis et al. 2014), and to account for the feedbacks and sudden shifts they can generate, thus requires understanding how the interaction structure of a community might change with shifting size structure.

Such changes in size-structure have been well documented on the Scotian Shelf, where the average aggregate body size of the fish community has declined substantially over recent decades, eroding macroecological patterns that have historically structured the region (Fisher et al. 2010a). These changes were driven by the collapse of cod and other large-bodied species, the subsequent trophic cascade (Frank et al. 2005), and widespread intraspecific shifts in species' size distributions (Fisher et al. 2010a). The loss of large-bodied individuals and the functional roles they occupied has likely restructured the interaction patterns of the Scotian Shelf fish community. Specifically, the loss of large individuals may have eroded the functional position of formerly dominant predators like cod, and changed their relationship with their forage fish prey. These changes in the interaction structure on the Scotian Shelf may serve to reduce the system's stability (Fisher et al. 2010a), and potentially slow cod recovery despite the moratorium on fishing declared in 1993 (Frank et al. 2005, 2011).

Understanding the dynamics of the Scotian Shelf fish community thus requires understanding underlying changes in its interaction structure. Multivariate autoregressive (MAR, or frequently vector autoregressive) models provide an accessible way to infer the drivers and structure of community dynamics (Hampton et al. 2013). As shown by Ives et al. (2003), the MAR model can be viewed as a first-order linear approximation to a more complex non-linear community model and thus offers insights into system stability. Further, MAR models fit the need for “models of manageable complexity” required for ecosystem based fisheries management (Lindegren et al. 2009). As such, these models have been used to explore the dynamics (Lindegren et al. 2009, Mac Nally et al. 2010, Francis et al. 2014) and dimensionality (Zhou et al. 2016, Thorson et al. 2017) of aquatic communities and to evaluate the effect of different management regimes (Lindegren et al. 2009).

In this study, we employed the MAR framework to model changes in the net sign and strength of interspecific interactions and expanded the framework to quantify those interactions as a function of the average lengths of the species involved. This approach provides a method for capturing the consequences of changing size structure (e.g., due to the loss of large individuals or changes to the underlying growth regime) for the interaction structure and stability of a system. We were particularly interested in identifying how the interactions between cod and the forage species have changed as both cod population and average length declined. We further explored the implications of the changing interaction structure for both cod recovery and system stability.

3.2 Methods

3.2.1 Data

We made use of data from annual July-August fisheries-independent bottom-trawl surveys conducted by the Department of Fisheries and Oceans Canada from 1970 to 2003 (Frank et al. 2005, 2011). These data provide average catch per tow (i.e., abundance per sampling unit) in either 3 cm length bins (predator species) or 1 cm length bins (forage species) for the two dominant large-bodied predator species (Atlantic cod *Gadus morhua*, and haddock *Melanogrammus aeglefinus*), and two forage species (herring *Clupea harengus*, and northern sand lance *Ammodytes dubius*). Although changes were observed across the Scotian Shelf community over this period, these four species represent the key players in the trophic cascade and subsequent system reorganization. We used the catch at length data to compute time series for the total catch per tow for each species, capturing each species' overall population dynamics, and time series of the average length of each species, capturing changes in each species' length distribution and functional make-up.

Cod and haddock were both commercially exploited, until a moratorium was declared on directed fishing in 1993, while exploitation of the forage fish was low (herring), or zero (sand lance) (Frank et al. 2011). As noted above, there was a widespread decline in the abundance of many of the predator species over the time period, and a dramatic collapse of cod in the late 1980s and early 1990s (Figure 3.1). Consistent with a trophic cascade (Frank et al. 2005), observed forage

fish abundance increased substantially after 1993, with very low, frequently zero, observed abundance prior to that (Figure 3.1). At the same time, the average length of all species broadly declined over the course of the time series.

3.2.2 Data model

Let y_{it} be the total average catch per tow for species i in year t . These observations are positive, continuous, and include zeros during years in which a species goes completely unobserved in the survey. To account for these features and maintain the proper support for the data, we employed a tobit link function (Clark et al. 2017, Taylor-Rodriguez et al. 2017):

$$y_{it} = \begin{cases} 0 & \text{if } v_{it} \leq 0 \\ v_{it} & \text{if } v_{it} > 0 \end{cases}$$

which allowed us to model the relationships among species on the natural (rather than log) scale, and account for zeros in the data by censoring negative latent abundance measures (Clark et al. 2017).

3.2.3 MAR del mar

Following the general framework of Hampton et al. (2013), we modeled the dynamics of the unconstrained v_{it} as:

$$\mathbf{v}_t = \mathbf{a} + \mathbf{B}_t \mathbf{v}_{t-1} + \mathbf{C} \mathbf{u}_t + \boldsymbol{\epsilon}_t$$

where \mathbf{B}_t gives the interaction matrix associated with year t , \mathbf{u}_t is a vector of external covariates, here bottom temperature anomalies, \mathbf{C} is an S by 1 vector of species coefficients mapping those covariates to species responses, and lastly system noise is modeled as

$$\epsilon_{it} \sim \text{Normal}(0, \sigma_i^2).$$

3.2.4 Gaussian process regression for interaction matrices

We assumed that the coefficient for each species’ effect on itself (i.e., the diagonal elements of the \mathbf{B}_t , often interpreted as a measure of density dependence) was constant, while we allowed the off-diagonal elements to vary through time:

$$B_{ijt} = \begin{cases} \beta_{ijt} & \text{if } i \neq j \\ \eta_i & \text{if } i = j \end{cases}$$

We hypothesized that the net strength of a given interspecific interaction is a function of the average lengths of the two species involved in the interaction (i.e., $\beta_{ijt} = f(x_{it}, x_{jt})$, where x_{it} is the average length of species i in year t). This function defines an interaction landscape, or surface, for the system. The average lengths of any pair of species, a “source” species and a “target” species, define a point on this surface that determines the effect of the source species on the target species. Thus, as species’ average lengths change, the locations of their interactions on this surface change, and the overall interaction structure of the system changes.

We modeled this surface using Gaussian process regression, in which all of the β_{ijt} were specified jointly as multivariate normal:

$$\text{vec}(\boldsymbol{\beta}) \sim \text{MVN}(\mathbf{0}, \boldsymbol{\Sigma}),$$

where the vector on the left-hand side stacks all of the $T * S * (S - 1)$ annual interspecific interaction coefficients and $\boldsymbol{\Sigma}$ is the covariance matrix. Thus every element k of $\text{vec}(\boldsymbol{\beta})$ represents the interaction coefficient between two species in a particular year, with corresponding vector \mathbf{x}_k containing the smoothed average lengths of those two species in that year. The covariance between interaction coefficients $\text{vec}(\boldsymbol{\beta})_k$ and $\text{vec}(\boldsymbol{\beta})_l$, Σ_{kl} , is defined as a function of the distance between \mathbf{x}_k and \mathbf{x}_l :

$$\Sigma_{kl} = \sigma_B^2 \exp\left(-\frac{1}{2\rho^2} \|\mathbf{x}_k - \mathbf{x}_l\|^2\right) + \delta_{kl}\tau^2,$$

where σ_B^2 defines the overall variance, ρ defines the length scale, δ_{kl} is a delta function that is 1 if $k = l$ and 0 otherwise, and τ^2 is a fixed noise term that ensures Σ is positive definite. The squared exponential covariance function produces an interaction surface where the interaction coefficient between any two species changes smoothly as a function of those species' average lengths.

3.2.5 Implementation

We embedded the MAR process model and the Gaussian process regression in a Bayesian hierarchical framework to carry out inference. We completed the specification of this model by assigning priors to \mathbf{a} , \mathbf{C} , $\boldsymbol{\sigma}$, $\boldsymbol{\eta}$, ρ , and σ_B , descriptions of which are given in the Appendix. We implemented this model in the Stan programming language (Carpenter et al. 2016), and used the 'rstan' package for R (R Core Team 2018, Stan Development Team 2019) to sample from the posterior distribution of the model parameters. We ran 3 chains with different starting values for 2,000 iterations each, discarding the first 1,000 as burn-in. Effective sample size, convergence diagnostics, and mixing were evaluated using the shinystan package (Gabry 2018). For every sample from the posterior distribution, we also simulated the one-step-ahead model predictions with \mathbf{B}_t held constant at its value in 1986, the year in which cod average length peaked, to explore how the predicted dynamics would have differed if species interactions had remained constant.

3.2.6 Stability analysis

Following (Ives et al. 2003), we computed stability quantities of the posterior mean \mathbf{B}_t to explore the consequences of the changing interaction structure for the stability of the system. The dynamics of a given system are stable (i.e., a long-term stationary distribution exists) if the magnitude of the dominant eigenvalue of \mathbf{B}_t , $\max(\lambda_{\mathbf{B}_t})$, is less than one. Given that the system is stable, the magnitude of the dominant eigenvalue provides a measure of the return time of the system to the stationary distribution following a disturbance, with larger values indicating systems with longer return times. Lastly, we compute the maximum system reactivity, given by $\max(\lambda_{\mathbf{B}_t^\dagger \mathbf{B}_t}) - 1$, as a measure of the short-term tendency of the system to amplify a perturbation.

3.3 Results

The MAR model was broadly able to describe the dynamics of these four species, though it was unable to fully capture some of the largest jumps in species abundance (e.g., the peak in cod in the early 1980s, and the relatively sudden jump in haddock, herring, and sand lance in the mid 1990s, Figure 3.1). Cod, haddock, and herring all exhibited very weak density dependence, with fairly large, positive estimates of η , while sand lance exhibited strong density dependence with an estimate of η near zero (Figure 3.4, the diagonal panels).

The Gaussian process regression framework allowed us to estimate an interaction surface defining the interaction strength between each pair of species in each year as a function of those species' average lengths in that year (Figure 3.2). The smoothness of this surface, i.e., how quickly the predicted interaction strength changes with changes in species' average lengths, is controlled by the effective length scale, ρ . Very small values of ρ would indicate that interactions are more independent, leading to a noisier, more rapidly fluctuating interaction surface. The posterior mean estimate of ρ was approximately 7 cm, indicating relatively low frequency fluctuations in interaction strength with the lengths of the interacting species (Figure 3.2).

Each interaction between each pair of species traced out a trajectory on this surface as the average lengths of each species changed. The arrows in Figure 3.2 provide an example of a portion of the trajectories traced by the cod-sand lance interactions. These arrows show that the effect of sand lance on cod was positive in 1986, but declined to negative by 2002. Conversely, the effect of cod on sand lance was negative in the 1980s, but shifted to a very weak positive interaction by 2002 (Figure 3.2, solid arrow).

Snapshots of the full interaction structure in 1986 and 2002 (corresponding to the years of the maximum and minimum cod average length) highlight the overall compression of the interspecific length distribution and the resulting changes in structure (Figure 4.7, with full time series given in Figure 3.4). In addition to the reversal in the interaction between cod and sand lance discussed above, we see that the initially positive effect of herring on cod disappeared by 2002. The effect of haddock on the other species was initially weak, but shifted to a strong positive effect on herring

and sand lance and a weak negative effect on cod. Herring had a weak effect on haddock for most of the time period, but shifted to a positive effect in the late 1990s and early 2000s. Lastly, the effect of cod on haddock and herring, the effect of herring on sand lance, and the effect of sand lance on haddock and herring all remained relatively constant through time (Figure 3.4).

Holding this interaction structure constant from 1986, when cod was at its largest average length, the effect of herring and sand lance on cod was positive, and the effect of cod on sand lance was negative, we predicted cod abundances much higher than their observed or fitted values from the late 1990s through the early 2000s (Figure 3.1, dashed line). In this scenario, we further predicted much lower abundances of sand lance in the early 2000s, and moderately lower abundances of herring and haddock (Figure 3.1, dashed line). It is important to note that these are one-step-ahead predictions. Thus, B_{1986} predicts that cod abundance would increase, even starting from the low values observed after the collapse.

The magnitude of the dominant eigenvalue of the posterior mean of each B_t fluctuated through time but was low through much of the 1980s, then increased in the early 1990s before dipping and increasing more dramatically in the late 1990s (Figure 3.5). The system's maximum reactivity also fluctuated through the first 20 years of the time series, but remained low through the early 1990s before increasing substantially beginning around 1995 (Figure 3.5).

3.4 Discussion

3.4.1 Summary

We found substantial variation in the interaction structure of the Scotian Shelf from 1970 to 2003. Further, the Gaussian Process regression framework that we developed allowed us to map this variation to changes in each species' average length. Notably, we found evidence of a switch in the signs of the cod-sand lance interaction from the expected +/- of a predator-prey interaction to a 0/- interaction as the average length of cod declined. These changes in interaction structure led to decreased system stability, and contributed to the explosion of forage fish abundance and the continued suppression of cod compared to simulations with a constant interaction structure based

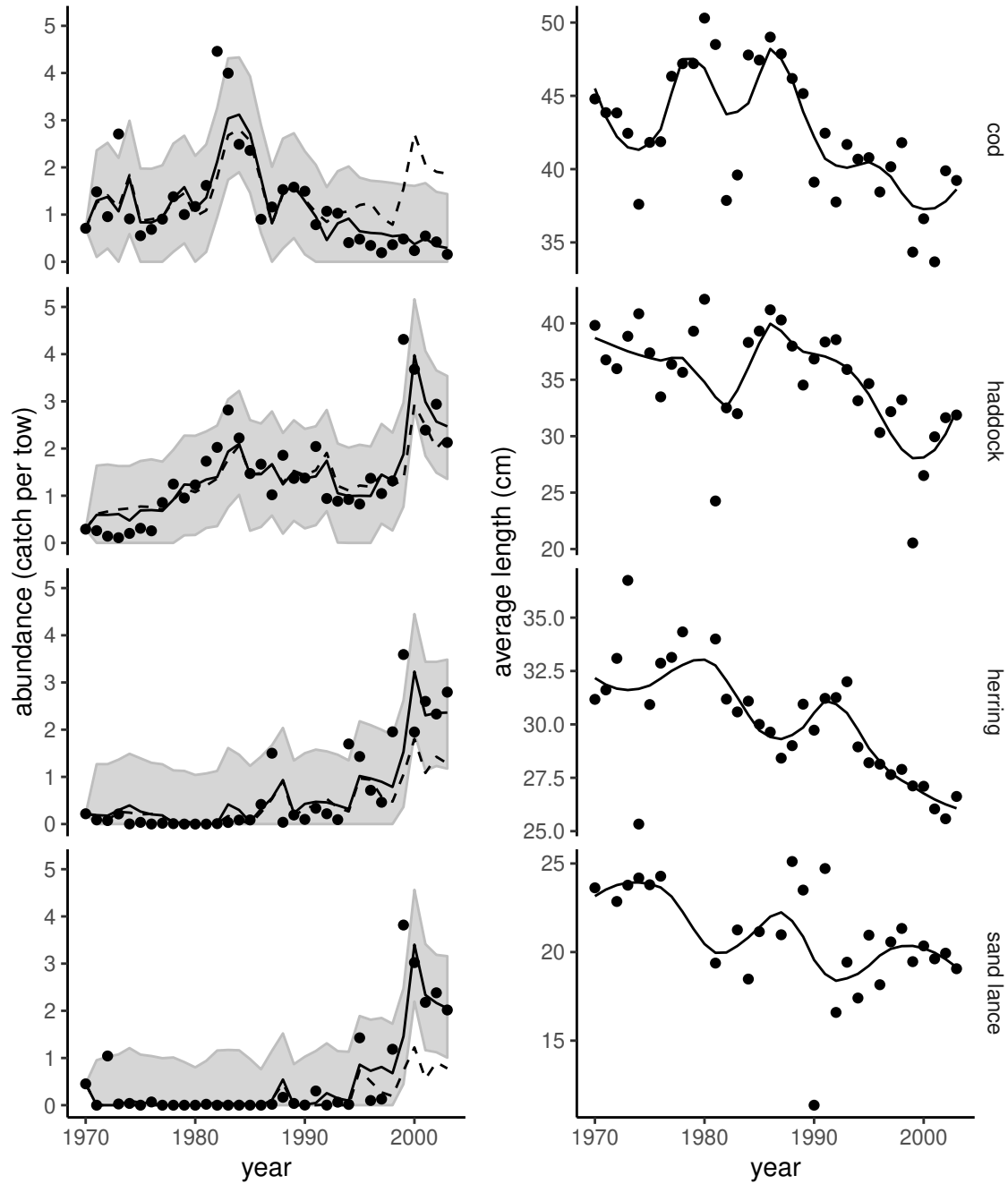


Figure 3.1: Abundance and average length trajectories for cod, haddock, herring, and sand lance. Left: the points indicate observed abundance (the y_{it}), the solid black line indicates the posterior median predicted abundance, and the gray ribbon indicates the 90% posterior credible interval. The dashed line represents the posterior median predictions holding \mathbf{B} constant at its value in 1986, when average cod length was largest. Right: the points indicate the observed average length and the black line indicates the *a priori* smoothed estimate (used to populate \mathbf{x}).

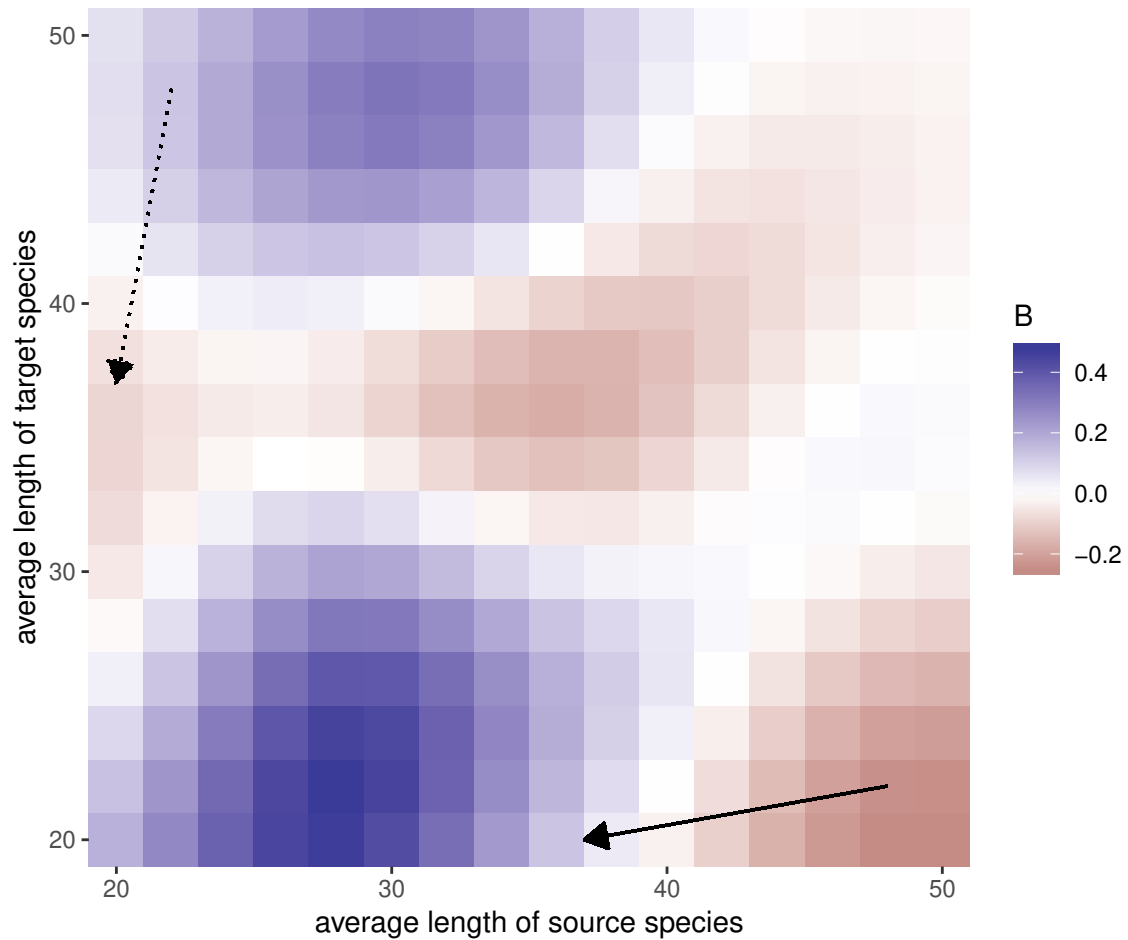


Figure 3.2: The posterior mean interaction surface as a function of the average length of the two species involved. The x-axis gives the average length of the source species (i.e., the species doing the influencing), and the y-axis gives the average length of the target species (i.e., the species being influenced). The arrows demonstrate the shift of the cod-sand lance interactions from 1986, the year of maximum average cod length, to 2002, the year of minimum average cod length. The solid line represents the effect of cod on sand lance, while the dashed line represents the effect of sand lance on cod.

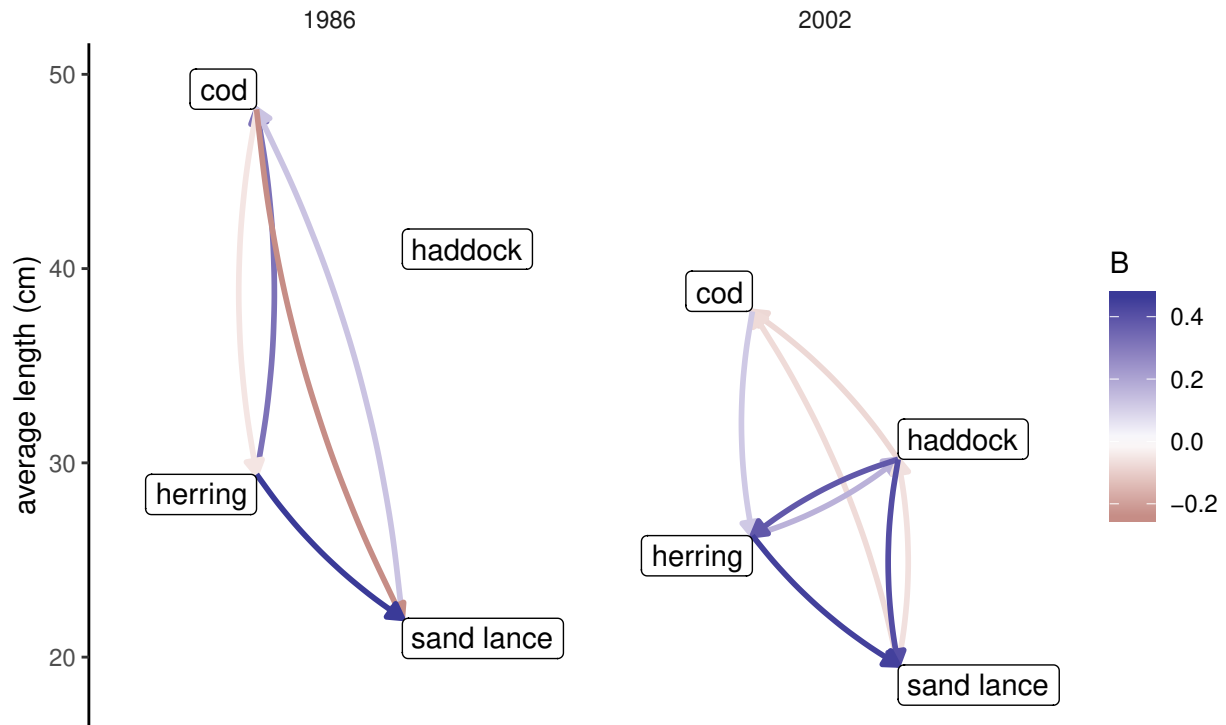


Figure 3.3: Snapshots of the interaction structure in 1986 (the year of maximum cod average length), and 2002 (the year of minimum cod average length). The position of each node on the y-axis indicates its average length in that year, arrows point from the source species to the target species and the color gives the posterior mean interaction strength. For clarity, interactions with an absolute magnitude less than 0.05 are not shown.

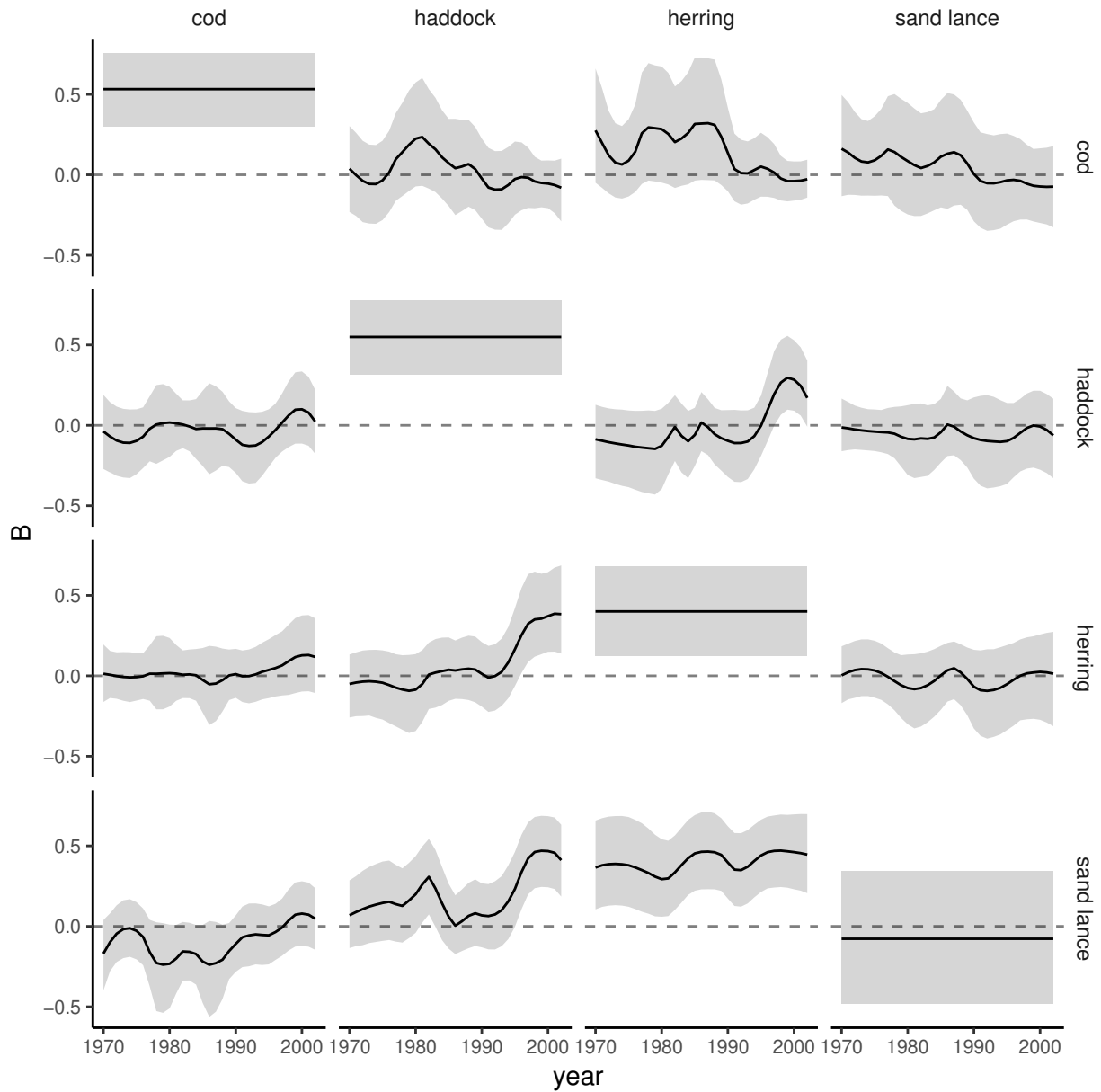


Figure 3.4: Posterior estimates of the pairwise interaction coefficients in each year (the B_{ijt}). The black line indicates the posterior median, while the gray ribbon indicates the 90% posterior credible interval. The panels on the diagonal represent each species' effect on itself, which we model as a constant (the η_i), apart from the Gaussian process regression.

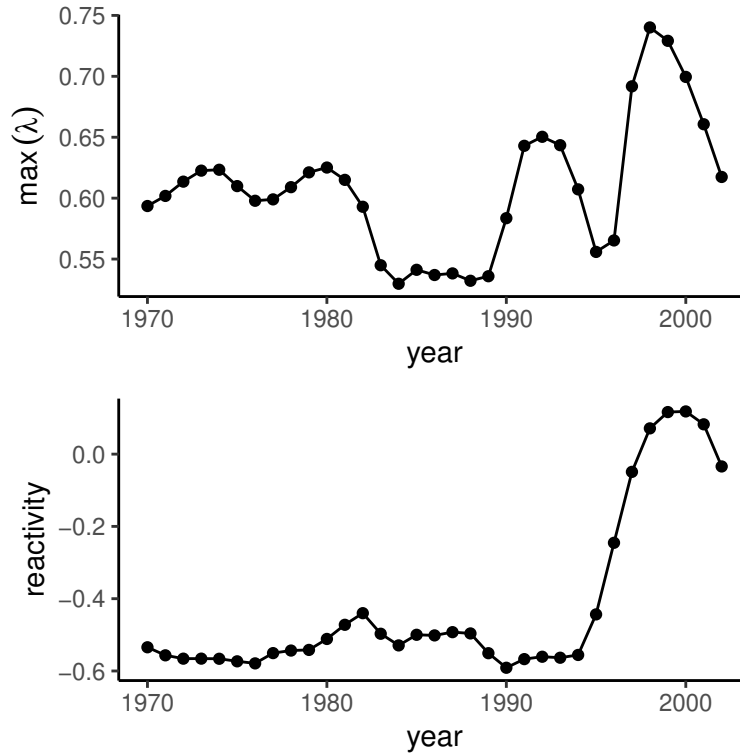


Figure 3.5: Stability quantities of the posterior mean \mathbf{B}_t . Larger values of $\max(\lambda)$, the magnitude of the dominant eigenvalue, correspond to longer return times following a perturbation. Larger values of reactivity indicate a tendency to initially amplify perturbations.

on the year of greatest average length for cod. Together, these results suggest that changes to the size-structure of these species were a major driver of the dynamics and stability of the Scotian Shelf ecosystem, extending beyond the changes apparent from shifts in abundance to shifts in the underlying interaction strengths that are fundamental to community organization.

3.4.2 Trophic cascade and loss of top-down control

The substantial changes in the interaction structure among cod, haddock, herring, and sand lance align with the observation that, following the collapse of the cod stock, the Scotian Shelf system shifted to a fundamentally different state (Bundy 2005, Frank et al. 2005). In addition to the changes in relative abundance resulting from the apparent trophic cascade (Frank et al. 2005), this new state was characterized in part by the loss of a top-down effect of cod on sand lance (Figure 3.4, indicated by the shift from a negative effect of cod on sand lance to a weakly positive effect). Modeling interaction strength as a function of species' lengths further revealed that this loss of control may be driven not just by the collapse of cod abundance, but also by its shrinking and shifting size structure.

Similar effects of declining size were observed on the Western Scotian Shelf, where, despite the relatively stable biomass of the predator complex, declines in predator body size were sufficient to initiate a trophic cascade and an increase in prey biomass (Shackell et al. 2010). The importance of the size distribution in determining the strength of predator-prey relationships may be driven in part by the fact that smaller individuals are simply less effective and efficient predators, due potentially to reduced burst swimming speed (Shackell et al. 2010). Moreover, the presence of ontogenetic niche shifts toward increased piscivory late in life-history mean that removal of large individuals may produce a disproportionate release in the predation pressure on a given forage fish species (Selden et al. 2018).

Thus, the presence of size-structure in a predator population means that a trophic cascade need not begin with a decline in predator abundance. However, when both size and abundance decline, the resulting trophic cascade is likely to be even stronger (Shackell et al. 2010). We see this

in our model's prediction that the forage fish boom would have been smaller had the community retained its size and interaction structure from the late 1980s, even given actual abundances (Figure 3.1). Even though cod persist in the system, our findings suggest that its size distribution has been truncated to the point that it is unable to occupy its former functional role relative to the forage fish in the community.

3.4.3 System stability

In addition to possibly initiating a new regime characterized by few cod and abundant forage fish, the estimated changes in interaction structure also initiated a shift in the stability regime of the Scotian Shelf (Figure 3.5). Both the dominant eigenvalues and reactivities marked an increase in instability from roughly 1995 on, suggesting a shift to a system with both slower return times following a perturbation and a tendency to amplify perturbations (Ives et al. 2003). These shifts in stability are consistent with the predictions of Fisher et al. (2010a) that the broad decline of body size in the Northwest Atlantic is likely to erode stability and generate a mismatch between the community size structure and the environment. Moreover, the link between the decline in average length and the increase in instability on the Scotian Shelf fits with findings from the California Current system linking fisheries-induced age (or size) truncation of a population to demographic changes that amplify nonlinear dynamics and variability (Anderson et al. 2008). Britten et al. (2014) similarly found a long-term decline in stability of the Ligurian Sea system concurrent with erosion of the top predator species and replacement with lower-trophic level species with faster life histories. These results, along with our own, highlight the important role that size structure can play in stabilizing both population and community dynamics and the risks posed by eroding that structure (Emmerson and Raffaelli 2004).

Though both measures of stability increased in the late 1990s, they followed different trajectories from 1990 to 1995, during which time the cod population was declining, but the forage fish had not yet responded. Specifically, the return time began to increase in 1990, while the reactivity remained relatively low, suggesting that return time began to react to the collapse and system

reorganization sooner than reactivity. Thus during this time period, the system response to perturbations was characterized by long asymptotic return times, but relatively rapid initial movement back toward equilibrium. The low reactivity during the early 1990s suggests that the collapse of the cod population may have strongly constrained system dynamics and limited the ability of stochastic perturbations to pull the system off its trajectory. This echoes results from measles modeling demonstrating a strong pull of stochastic perturbations back toward the attractor on the downswing of an epidemic (Grenfell et al. 2002). Thus the Scotian Shelf system provides an example of how a perturbation (i.e., the collapse of cod), and the loss of particular components of a community (i.e., large fish) can generate different responses in otherwise broadly similar measures of stability (Donohue et al. 2013).

Changes in the stability regime of the Scotian Shelf and the collapse of cod also highlight the increased risk of stochastic extinction, due both to the increased instability and fluctuations generated by the dominance of the forage fish population and to the low abundance of cod. This simultaneous increase in these two components of stochastic stability, termed σ -instability (i.e., instability due to large fluctuations) and μ -instability (i.e., instability due to low abundance) by Gellner et al. (2016), further highlights the multidimensional nature of stability. Frank et al. (2011) argue that the fluctuations in forage fish may be damping out due to competition, thus suggesting a potential decline in σ -instability in recent years. However, there has been relatively little indication of relief from the μ -instability due to low cod abundance.

Consistent with the characterization of μ -instability, multiple hypotheses for the continued low abundance of cod suggest that the system may be in an alternative stable state due to emergent Allee effects generated by the interactions between cod and the now dominant forage fish complex (Gårdmark et al. 2015). Modeling of so-called overcompensatory dynamics in forage fish suggests that, without sufficient predation by large cod, strong competition among forage fish can lead to reduced growth, poor condition, and weaker reproduction, leaving relatively few and/or poor quality prey available for cod predators (de Roos and Persson 2002, van Leeuwen et al. 2008). Our estimated decline in the positive effect of herring on cod provides support for this hypothesis,

suggesting that cod were unable to take advantage of the abundant herring prey. Moreover, by mapping species interactions onto their average lengths, our results further link overcompensatory dynamics to the length structure of herring and cod. The loss of the positive effect of herring on cod occurs along with a decline in average herring length, suggesting a decline in condition and quality of food available to cod (Frank et al. 2011). The average length of cod also declines over this time, suggesting that the largest cod were the ones most responsible for turning herring prey into more cod.

Closely related to the overcompensation hypothesis, the cultivation-dependence hypothesis suggests that competition between juvenile cod and now abundant forage fish, as well as potential predation by forage fish on cod eggs and larvae, may induce a bottleneck in the growth and survival of juvenile cod (Walters and Kitchell 2001, Bundy and Fanning 2005). Again, our estimates of the changing interaction structure on the Scotian Shelf provide empirical support for this hypothesis. Specifically, we identified a shift in the effect of sand lance on cod from positive to negative (Figure 3.4). Thus, with abundant forage fish, and a lack of large cod able to control those forage fish, cod abundance may remain at low levels, maintaining persistently high stochastic extinction risk.

3.4.4 Cod recovery and management

Our model is unable to fully distinguish between an alternative stable state or a prolonged transient, but our results do suggest that the potential for population recovery is bound up with recovery of the former length distributions. Fisher et al. (2010a) suggested that recovery of this historic size-structure may be hindered by intensified competition for resources among both forage fish and diminished predators. Our results suggest that a relaxation of this competition – and a restoration of the former interaction patterns – could help push the system toward recovery. It is possible that, as processes within the forage fish complex damp out their large fluctuations, this intensified competition will also damp out (Frank et al. 2011). Alternatively, management actions could be taken to reduce forage fish abundance. Counter-intuitive as it may be to try to boost cod by reducing their prey base, removing forage fish could reduce both inter- and intraspecific

competition and allow the size-structure of the forage fish populations to tilt more favorably for cod (de Roos and Persson 2002, van Kooten et al. 2005, van Leeuwen et al. 2008). If these changes restored the net interaction landscape to its historical structure, our results suggest that cod may be able to better take advantage of and control the forage fish complex and recover from low abundance (Figure 3.1, dashed line).

However, the late 1990s increase in the abundance of haddock suggests a possible reorganization of dominance in the predator complex, even in recovery (Frank et al. 2011). Haddock has more variable recruitment than cod, which possibly enabled it to capitalize on a chance good recruitment class in 2000 (Fogarty et al. 2001). Moreover, the emergence of stronger interactions between haddock and the rest of the system, including a negative effect of haddock on cod and a positive effect of herring on haddock, suggest that even if cod recovers, it may have forfeit its position as the dominant predator species.

3.4.5 Future work

The Gaussian process regression framework we developed allowed us to flexibly connect changes in species interactions to observed changes in species average lengths and to estimate the underlying interaction landscape on which species moved. This framework revealed that the prospects for cod recovery are closely linked to length-structure. Thus, better understanding the potential for recovery may require better understanding the feedbacks between population dynamics and length dynamics. For instance, we might expect that a lack of suitable forage fish prey, or competition between juvenile cod and sand lance might work to suppress cod growth and the recovery of large individuals. Moreover, identifying the top-down effects of cod on the length structure of forage fish prey could be particularly important for further evaluating the cultivation-dependence hypothesis (de Roos and Persson 2002, van Leeuwen et al. 2008). Including species average length as a dynamic state variable along with species abundances in the MAR framework might offer a tractable way forward, without needing to fully resolve size-structured community dynamics (e.g., Hartvig et al. 2011).

Our focus was on just four species: the two dominant large-bodied predators, and the two forage species for which relatively consistent data are available. These species represent the dominant species before and after the collapse (Frank et al. 2011), and thus likely account for a disproportionate amount of the dynamics. Moreover, the use of more tractable modules to gain insight into the structure and stability of broader food webs is well established (Bascompte and Melián 2005, Bascompte 2009). However, including additional components of the Scotian Shelf community may help to better parse the observed system changes. In particular, the model could be extended to include additional trophic levels, for example zooplankton (whose abundance may drive competition among forage fish; Frank et al. 2011) or grey seals (who may exert top-down control over the cod population; O’Boyle and Sinclair 2012). Further, including benthic macroinvertebrates may be particularly interesting due to their simultaneous release from predation along with forage fish (Bundy 2005) and the potential stability consequences of the balance between benthic and pelagic energy channels (Rooney et al. 2008).

3.4.6 Conclusions

Our findings highlight that the dimensions of system stability often evolve dynamically along with species abundance (Ushio et al. 2018), and that the relationships among species in a community can change, even if species richness does not (McConkey and O’Farrill 2015). In particular, the presence of distinct functional components – with distinct interaction patterns – within a species’ life history means that interspecific interactions and community stability are closely tied to the size-structure of the constituent species. The loss of large individuals can have especially profound consequences that can ripple through the growth and mortality regimes of the community and alter the resulting landscape of interspecific interactions. The success of efforts to maintain and restore exploited ecosystems thus hinges on the ability of management actions to maintain and restore the community’s size-distributions, and the full functional diversity they contain (Fisher et al. 2010b).

Chapter 4

Food web structure of ontogenetic niche shifts

4.1 Introduction

Food webs provide ecologists with a map of the routes through which energy flows in a community (de Ruiter et al. 1998, Cohen et al. 2003, Rooney et al. 2008). However, these maps are often complex and their essential features difficult to identify. Understanding food web structure is further complicated by the presence of intraspecific variability in both resource use (Bolnick et al. 2003) and enemies. For many species (e.g., amphibians, aquatic insects, and fish) this variability in predators and prey is structured by ontogenetic development (Werner and Gilliam 1984). The presence of these ontogenetic niche shifts mean that individuals of a species frequently do not occupy a single fixed role in the food web, but rather move through a landscape of roles as they grow (Werner and Gilliam 1984, Muñoz and Ojeda 1998, Garrison and Link 2000).

The particular structure of ontogenetic niche shifts in a community can have substantial consequences for the community's dynamics and stability. Ontogenetically structured models suggest that the outcome of predator-prey interactions (e.g., top-down control, or exclusion of either the predator or prey) depends on both the number of niche shifts in the predator's life history (van Leeuwen et al. 2013), and whether those niche shifts are complete or nested (i.e., whether the niche shift represents the addition of new prey types or a complete shift in prey; Hin et al. 2011, van Leeuwen et al. (2014)). Further, the presence of ontogenetic niche shifts means that species that appear as generalists may in fact be ontogenetic specialists, with each stage specializing on a particular resource (Rudolf and Lafferty 2011). The reliance of particular stages of predator life history on relatively specialized sets of resources means that food webs may be considerably less robust to species loss than indicated by studying aggregate resource use at the species level (Rudolf and Lafferty 2011). Thus the extent of specialization of the ontogenetic niches that make up a food web can have important consequences for our understanding of community stability.

The importance of understanding the structure of ontogenetic niche shifts, both within a species and across the food web, highlights the need for more individual-based perspectives on food web structure. At the same time, considering all the interactions among all the distinct stages of every species (Polis 1984) risks substantially increasing the dimension of the predator-prey arena without clearly distinguishing the different roles that individuals might occupy. Thus, describing the ontogenetic structure of a food web requires both an individual-level perspective and a method for reducing the dimension of the resulting trophic complexity by identifying patterns of trophic similarity among the constituents of the community (Yodzis and Winemiller 1999). Along these lines, Allesina and Pascual (2009) suggest that food web structure can be best modeled by partitioning species into trophic groups: collections of species that have similar predator-prey relationships with other groups. When applied to a well-resolved food web of the Serengeti, Baskerville et al. (2011) found that the trophic groups model provided a reduced-dimension description of the food web that revealed spatial partitioning and multiple channels of energy flow.

Applied to an individual-level, or ontogenetically resolved, food web, trophic groups offer a way to identify the trophic roles that partition a species, and the community, into its distinct ontogenetic niches. However, the trophic group models of Allesina and Pascual (2009) and Baskerville et al. (2011) lack a mechanism for informing the identification of trophic groups with additional biological information beyond just the food web. Given the information contained in the inherently hierarchical structure of ontogeny (individuals belong to a species and a position along an ontogenetic axis), and the role that structure may play in determining the trophic position of an individual, richer models are required to understand the ontogenetic signal in trophic groups.

Understanding how the distinct trophic niches of a community are partitioned is especially important in marine fisheries systems where individual trophic level is strongly correlated with size (Jennings et al. 2002, Marsh et al. 2015), fishing is often size-selective (Zhou et al. 2010), and food web frameworks are needed to inform ecosystem based fisheries management (Travis et al. 2014). At the same time, fisheries agencies, such as the Alaska Fisheries Science Center (AFSC) of NOAA, frequently collect well-resolved datasets of predator stomach contents that offer a unique

opportunity to examine food web structure at the level of individual predators and prey. The Gulf of Alaska represents a particularly interesting system in which to explore the ontogenetic structure of the food web due to its dominance by a core collection of apparently generalist predators with large size ranges (Gaichas and Francis 2008, Gaichas et al. 2015) and the importance of walleye pollock as both predator and prey (Gaichas et al. 2015).

In this study, we developed a framework for incorporating additional biological information, for example, the states or traits of the nodes in the food web, into a trophic groups model. By modeling these additional features alongside the foodweb, this framework offers insights into the patterns of trophic group partitioning across those added dimensions. In particular, this framework reveals the extent to which trophic groups – collections of nodes with that are homogeneous in their interaction patterns – are also homogeneous across the added biological dimensions. We applied this framework to an ontogenetically resolved food web for the Gulf of Alaska, where we added species identity and size as the additional factors that we expected to covary with trophic group membership. This allowed us to better describe the core features of the Gulf of Alaska food web, the unique (or not) roles played by different components of different species, and the major avenues through which energy flows in the community.

4.2 Methods

4.2.1 Stomach contents data

The AFSC stomach contents database (Livingston et al. 2017) contains 17,089 predator-prey records from 5,943 predator stomachs collected from the Gulf of Alaska between 1981 and 2009. Each of these records provides both predator and prey species (where prey were identifiable), as well as predator and prey length (when prey were intact enough to measure). Predator length is measured to the nearest 1cm, while prey length is measured to the nearest 1mm.

The database contains records for 38 species of predator and 108 species of prey. However, sampling is highly skewed toward a core set of predators of ecological and commercial interest. As such, we restricted our analysis to include the five most sampled predator species (arrowtooth

flounder *Atheresthes stomias*, Pacific halibut *Hippoglossus stenolepis*, Pacific cod *Gadus macrocephalus*, walleye pollock *Theragra chalcogramma*, and sablefish *Anoplopoma fimbria*), and the five most frequently observed prey species (walleye pollock *Theragra chalcogramma*, capelin *Malotus villosus*, Tanner crab *Chionoecetes bairdi*, sand lance *Ammodytes hexapterus*, and pygmy cancer crab *Cancer oregonensis*). Interactions among these nine species represent 85% of the observed records. We assembled the food web by binning each species into 2 cm size bins (to smooth over heterogeneity in sampling effort), defining each of these bins as a node, and counting the number of times each prey was observed in the stomach of each predator.

4.2.2 Bento box process model

The model developed here can be applied generally to any food web with additional biological information on node attributes. However, given the central role of the Gulf of Alaska system in our motivation and development, we name this model the “Bento box process,” given its goal of apportioning slices of fish to different compartments. In the trophic groups framework (Allesina and Pascual 2009, Baskerville et al. 2011), or equivalently in a stochastic block model (Nowicki and Snijders 2001), we assume that interactions can be described by partitioning the food web’s nodes into K groups such that the interaction probability among any two nodes is determined by their group membership. Let y_{ij} indicate the number of stomachs collected from predators of species s_i and log-length x_i that contained prey of species s_j and log-length x_j . Then,

$$y_{ij} \sim \text{Binomial}(J_i, \phi_{z_i z_j})$$

where J_i is the number of stomachs collected from predator i , z_i gives the group membership of node i , and ϕ is a K by K matrix of pairwise interaction probabilities between groups. Other formats for food web data (e.g., binary observations) can be easily accommodated by swapping out the binomial model above for the appropriate measurement model (e.g., Bernoulli).

We expected trophic groups to be defined not just by the interaction patterns they generate, but also by the size distribution and species composition of the constituent nodes. Following the

spatial clustering model of Reich and Bondell (2011), we incorporated this additional information by modeling the length and species identity of each node jointly with the interaction structure as a function of its latent group membership:

$$x_i \sim \text{Normal}(\mu_{z_i}, \sigma_{z_i}^2),$$

and

$$s_i \sim \text{Categorical}(\boldsymbol{\theta}_{z_i}),$$

where μ_k and σ_k^2 define the length distribution of group k and $\boldsymbol{\theta}_k$ defines the species composition of group k . Modeling species and length jointly with the trophic groups allowed us to account for additional node-level information and forces the model to balance partitioning the interactions with creating groups of homogeneous length and species identity.

Rather than choose the number of groups K *a priori*, we modeled the group assignments with an infinite mixture model (Reich and Bondell 2011, Johnson et al. 2013, Brost et al. 2017, Johnson and Sinclair 2017). This allowed the data to select the appropriate number of groups. In this framework, the group membership of node i is determined by:

$$z_i \sim \text{Categorical}(\boldsymbol{q}).$$

The q_j (i.e., the group membership probabilities) were modeled with a stick-breaking prior, such that

$$\begin{aligned} q_1 &= U_1 \\ q_j &= U_j \prod_{k=1}^{j-1} (1 - U_k) \\ U_k &\sim \text{Beta}(1, \beta) \end{aligned}$$

where β controls the sparsity of the prior (i.e., the number of groups in which the membership probability accumulates). The group membership probabilities must sum to one, so moving in

order, each q_j is defined as the fraction of the remaining probability space that it claims (i.e., U_j gives the fraction of the remaining stick that is broken off and assigned to q_j).

4.2.3 Priors

We specified hierarchical priors on the parameters of the mixture components, such that:

$$\phi_{jk} \sim \text{Beta}(a_\phi, b_\phi)$$

$$\mu_k \sim \text{Normal}(\mu_0, \sigma_0^2)$$

$$\sigma_k^2 \sim \text{InverseGamma}(a_\sigma, b_\sigma)$$

$$\theta_k \sim \text{Dirichlet}(\gamma).$$

We used uninformative priors for the ϕ and μ , but informative priors for the σ^2 and θ , to allow groups with large species diversities or size ranges only when well-supported by the stomach contents data.

We modeled the concentration parameter of the infinite mixture with a gamma prior:

$$\beta \sim \text{Gamma}(a_\beta, b_\beta),$$

with a_β and b_β chosen to favor relatively few groups, based on the tests of Reich and Bondell (2011).

4.2.4 Implementation

To facilitate sampling, we truncated the infinite mixture model at a finite number of components, in this case, 30 (Reich and Bondell 2011). We used Markov Chain Monte Carlo to draw samples of all model parameters from their posterior distributions. Though the z_i can be sampled sequentially from their conditional distributions using Gibbs updates, to improve mixing, we implemented the split-merge sampler of (Jain and Neal 2007) that can generate large changes in group assignments and prevents the sampler from getting stuck in local modes. We paired this

with Gibbs updates of all model parameters, taking advantage of conditional conjugacy to draw samples from closed-form conditional distributions.

Each draw from the posterior distribution represents a potentially different partition, with potentially different labels, i.e., a different \mathbf{z} , making summarizing the features of the groups difficult. To aid in this, we identified a single ‘consensus partition’ that best represented the posterior distribution (Dahl 2006, Reich and Bondell 2011). For every pair of nodes, we computed the posterior probability that they occupied the same group, such that D_{ij} gives the proportion of MCMC iterations in which $z_i = z_j$. Then we identified the consensus partition by identifying the MCMC iteration with the adjacency matrix ($A_{ij} = I(z_i = z_j)$) that was closest to the matrix, \mathbf{D} . Essentially, we found the single posterior sample that had the group partition that most closely matched the overall posterior probabilities that any two nodes occupy the same group (Dahl 2006, Reich and Bondell 2011).

4.3 Results

The interactions between every pair of predator and prey species can be summarized by an interaction surface over the plane defined by each species’ length range, with each point giving the probability that a prey of a given length appears in the stomach of a predator of a given length. Our model assigns these probabilities by assigning to each length-class of each species a latent group membership that indexes the appropriate ϕ . The resulting block-structure is clearly visible in the surface of the mean posterior interaction probabilities between arrowtooth flounder predators and pollock prey (Figure 4.1, see Appendix for all pairwise plots). The posterior interaction surface clearly partitions the length classes of arrowtooth flounder and pollock into areas of relatively high interaction intensity (e.g., 60 to 80 cm arrowtooth flounder feeding on 30 to 50 cm pollock) from those of relatively low (e.g., 20 to 60 cm arrowtooth flounder feeding on those same pollock). Overall, our inferred partitioning of each of these predator-prey surfaces successfully captured the observed prey counts, with the mean posterior predicted y explaining 83% of the variation in the observed y_{ij} (Figure 4.2).

Though the model was able to partition the food web into groups of nodes that were relatively homogeneous in their interaction patterns, the partitions generally contained a heterogeneous mixture of both species and lengths (Figure 4.3). If every group was uniquely associated with a single length class, the posterior estimates of the μ_{z_i} would closely match the observed x_i . On the other hand, if groups were partitioned randomly with respect to length, the μ_{z_i} would capture very little of the observed x_i . We found that the Gulf of Alaska system falls between these two extremes, indicating clear separation of groups by size, but broad size ranges within those groups (Figure 4.3). Similarly, if the identified groups completely separated by species identity, the model would predict species labels very accurately (i.e., the posterior estimates of θ_{z_i, s_i} would be near one). On the other hand, if groups were not distinguished by species at all (i.e., if species identity offered no information on group membership), the posterior estimates of the θ_{z_i, s_i} would be small (i.e., around the inverse of the number of species). Again, we found that the Gulf of Alaska falls between these two extremes, indicating that most groups are shared by multiple species (with the exception of some groups unique to pollock, Figure 4.3).

The posterior distribution of the number of realized groups suggests that the food web assembled from the Gulf of Alaska stomach contents data could be partitioned into roughly 16 to 18 trophic groups (Figure 4.4). This is more groups than the number of species, but substantially fewer groups than the number of nodes. Examining the consensus partition, we found substantial overlap among the four top predator species, with sablefish and arrowtooth flounder occupying the same sequence of two groups, cod and halibut occupying the same sequence of three groups, and the largest size classes of all four of species occupying the same trophic group (Figure 4.5). This group of large predators (group 17) was distinguished primarily by being the only group to prey on 30 - 50 cm pollock (group 15, Figure 4.6, Figure 4.7).

The distinction between the cod/halibut and sablefish/arrowtooth flounder groups can be seen in Figure 4.7 and Figure 4.6. Small sablefish and small arrowtooth flounder (group 14) were characterized by feeding primarily on small forage fish (groups 8 - 10, 12), while the two groups occupied by cod and halibut (groups 13 and 16) had a diet of both crabs (primarily groups 2 and 4)

and forage fish, with the larger of the two groups (group 16) exploiting larger size classes of those prey types. Connecting the identified trophic groups that are linked by ontogenetic niche shifts highlights the role of growth in generating energy flow from otherwise top-predator groups (13, 14, and 16) to the largest individuals in group 17 (Figure 4.7).

The size classes of all the prey species were also split into multiple different groups (Figure 4.5). In many cases, these partitions reflected differences in the predators of different size classes of prey (e.g., the large size classes of Tanner crab were consumed by larger size classes of cod and halibut). Other partitions of the prey species reflected differences in overall interaction intensity or availability (e.g., groups 6 and 11 contain some of the smallest and/or largest size classes of prey species that are poorly represented in the data and thus have weak interaction probabilities, Figure 4.6).

Pollock, which is represented in the data as both predator and prey, was separated into the most trophic groups, overlapping with both the other prey species at its smallest sizes, and with sablefish and arrowtooth flounder at its largest sizes (Figure 4.5). Pollock between 30 and 50cm occupied a unique middle trophic level that was preyed upon by large predators and was itself a predator of several forage fish groups (Figure 4.7, group 15). The ontogenetic trajectory of pollock (beginning in group 3 and ending in group 14) demonstrates how much of the food web an individual traverses over the course of its ontogeny (Figure 4.7). Lastly, as a caveat, group 12 corresponds to the small pollock, for which relatively few stomachs were collected. As such, the model overestimates the generality of its diet (i.e., no crab were observed in the diet of small pollock, but there were not enough stomach samples to rule them out, Figure 4.7, Figure 4.6).

4.4 Discussion

4.4.1 Summary

The bento box model identified a low-dimensional description of the ontogenetically resolved Gulf of Alaska food web. This dimension reduction allowed us to more easily trace the ontogenetic trajectories followed by individuals in the system, and the routes by which those trajectories carry

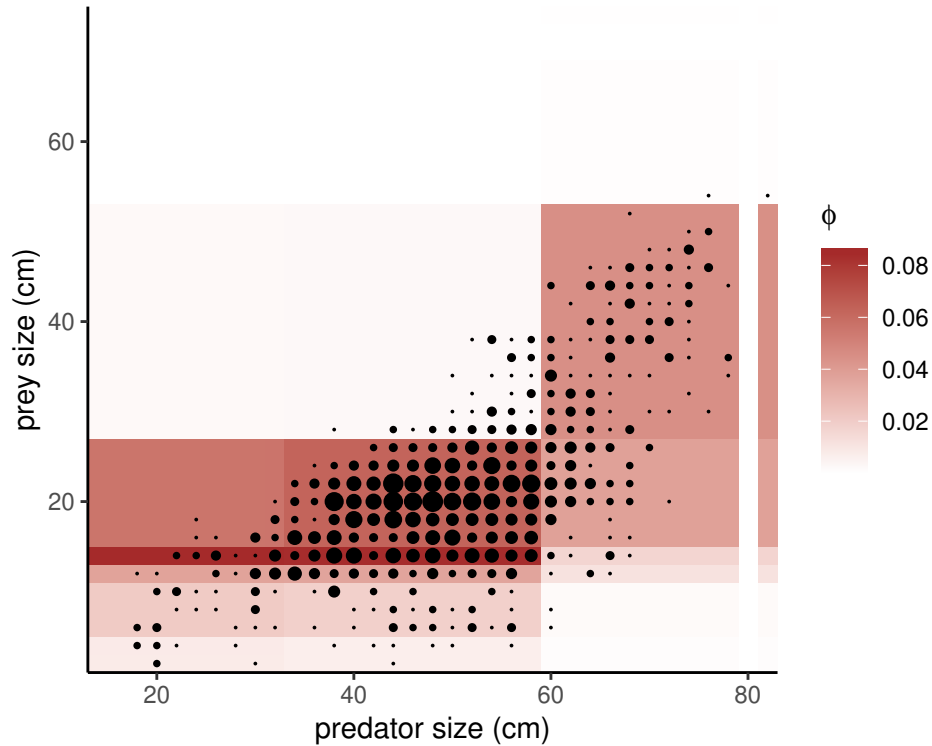


Figure 4.1: Posterior predicted interaction surface between pollock prey and arrowtooth flounder predators. The red shading indicates the mean posterior interaction probability (ϕ) between every length of predator (x-axis) and prey (y-axis). The points indicate the observation of a prey item in the stomach of a predator, with the size of the point indicating y , the number of predator stomachs in which that prey was observed. A full plot of all predator and prey species is available in the appendix.

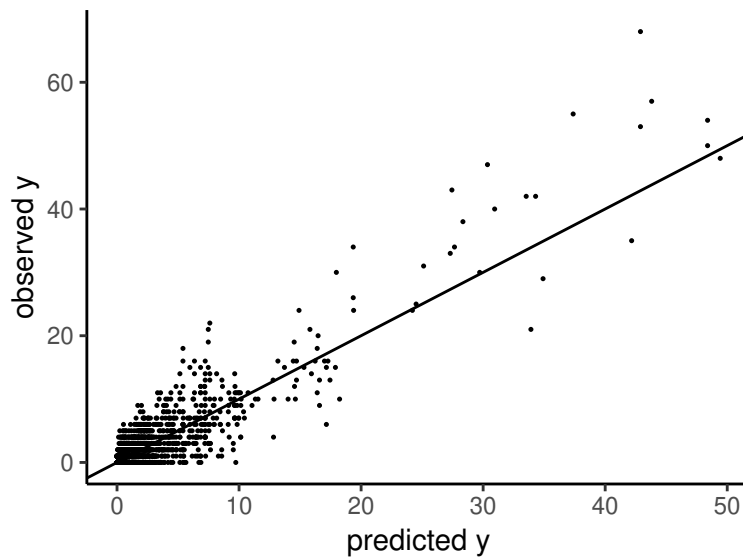


Figure 4.2: The observed counts of prey in predator stomachs (the y_{ij}) plotted against the mean posterior expected counts ($\phi_{ij} J_i$). The line indicates the 1:1 line.

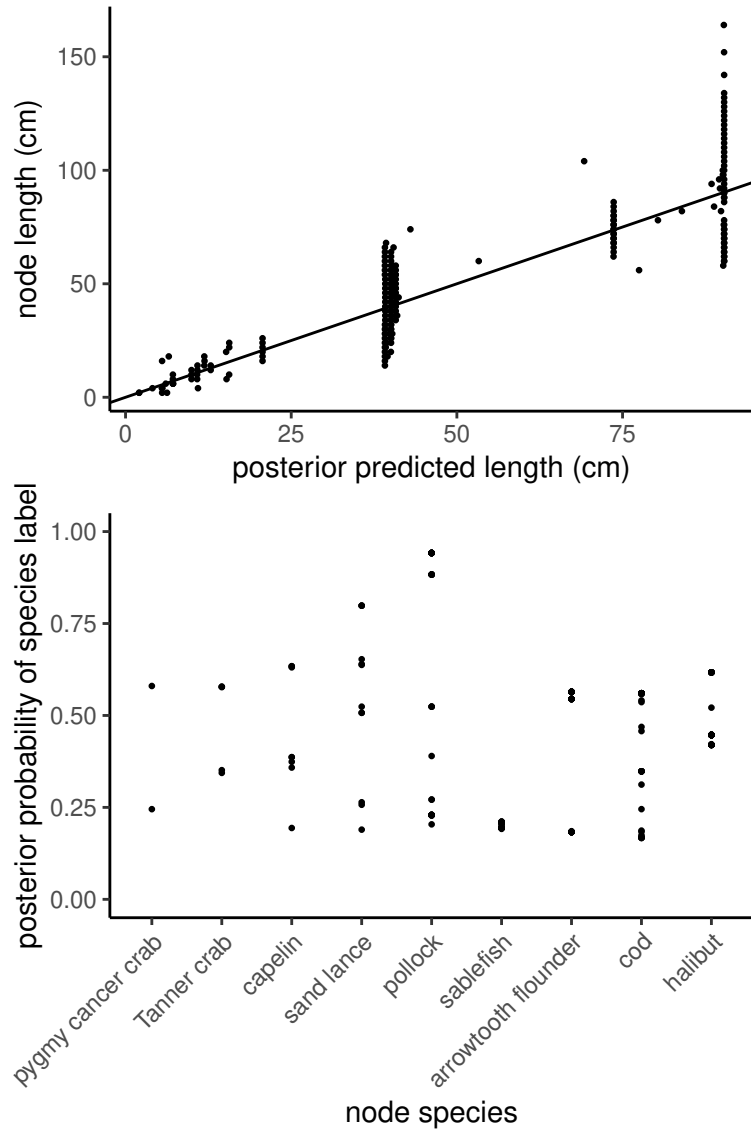


Figure 4.3: Model fits to node length (the x_i) and species identity (the s_i). The top panel plots the observed length of each node against its mean posterior predicted length (i.e., μ_{z_i}). The line indicates the 1:1 line. The bottom panel plots the mean posterior probability of each node's species label (i.e., θ_{z_i, s_i}).

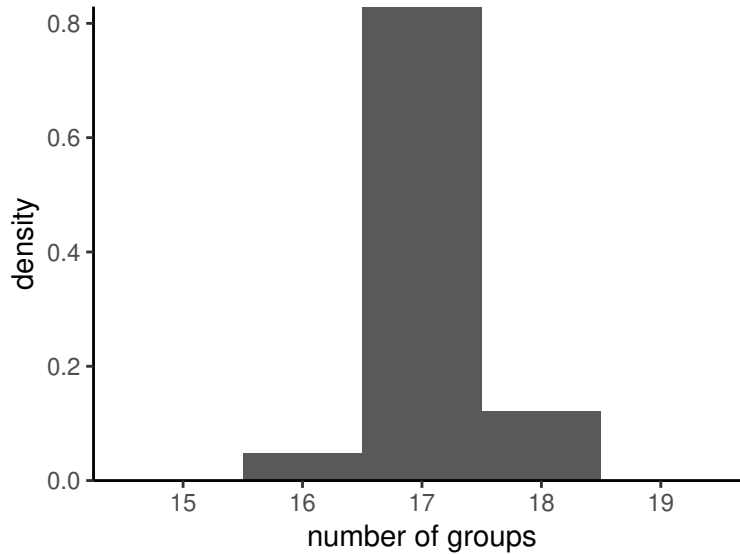


Figure 4.4: Posterior distribution of the number of trophic groups.

energy up the food web. In addition, modeling the partitioning of the food web jointly with a partitioning of node species and length revealed that group assignment generally mapped to broad distributions of both species and length. These findings reveal the shared ontogenetic backbone that ties the Gulf of Alaska community together and the mix of both ontogenetic development and predator-prey relationships that govern energy flow in the system.

4.4.2 The structure of the ontogenetic niche space

Following an individual across its ontogeny, the transitions from one trophic group to the next were driven largely by expansion of the diet, rather than a distinct shift in diet. We see this most clearly in the ontogenetic shifts of cod and halibut, across which most the previous prey were retained, with new items added (e.g., the addition of intermediate pollock in the shift from group 15 to group 17, Figure 4.7). This is consistent with other studies identifying an increase in diet breadth with size (Garrison and Link 2000, Scharf et al. 2000, Petchey et al. 2008, Williams et al. 2010) and the fact that predator diets tend to be nested, with an individual generally consuming a subset of the prey consumed by larger individuals (Woodward and Hildrew 2002). The identification of broad trophic groups, with relatively broad, nested diets suggests that these species are not

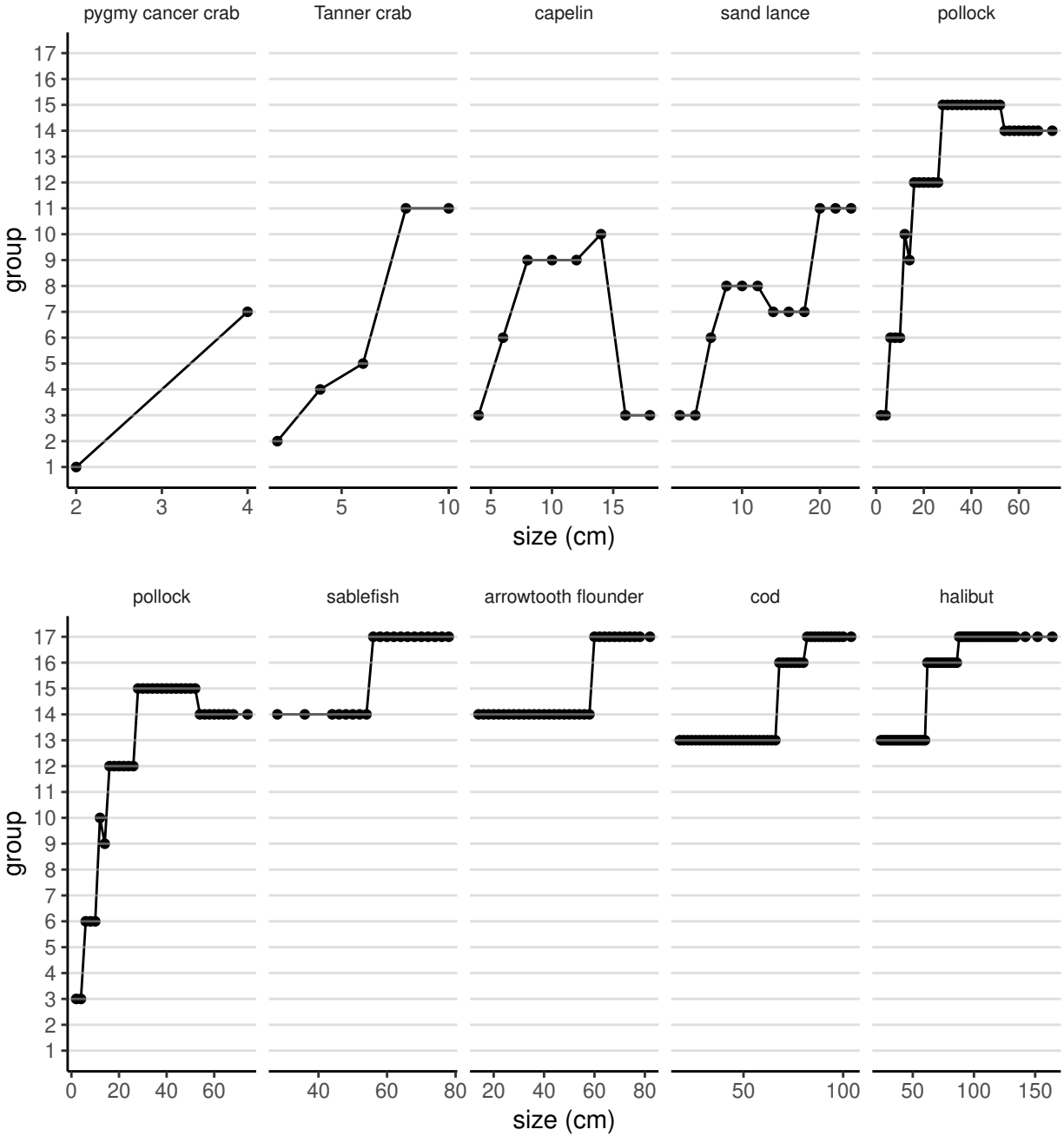


Figure 4.5: Group membership of every node in the food web, taken from the consensus partition (i.e., the posterior sample whose group assignments z produce the group adjacency matrix that is closest to the full posterior affinity matrix). The groups are ordered by their average size μ_k .

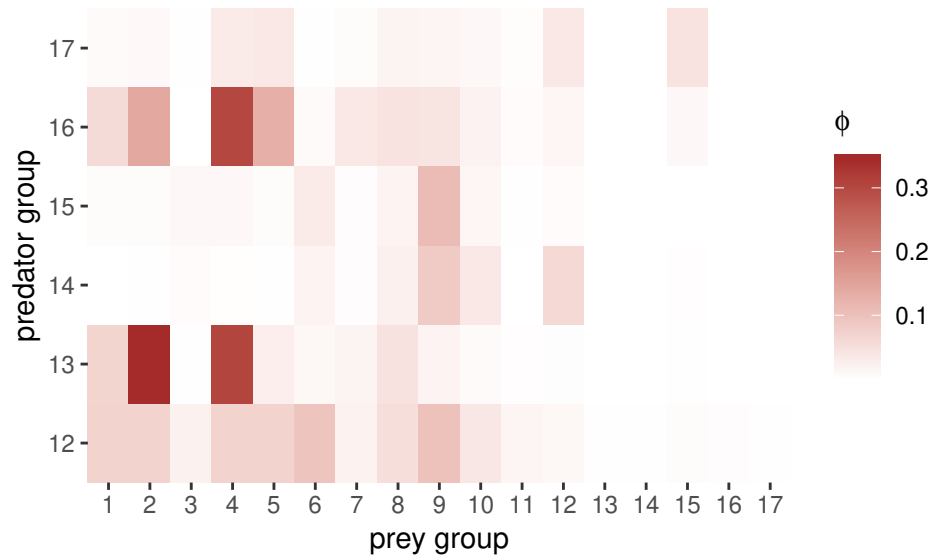


Figure 4.6: Group-wise interaction probabilities (the ϕ_{ij}) corresponding to the consensus partition. The shading of each cell represents the probability that a prey item in that column appears in the stomach of a predator in that row. The rows for groups containing only prey nodes were omitted.

generally ontogenetic specialists, and thus even the ontogenetically resolved food web may be relatively robust to species loss (Rudolf and Lafferty 2011).

In addition to overlap in the diets of the different trophic groups traversed by an individual, we also identified substantial overlap among the ontogenetic trajectories of Gulf of Alaska predators. Although previous studies have identified the same general trends of increasing piscivory (Yang et al. 2006) and trophic level (Marsh et al. 2015) with size, our analysis revealed that there is relatively little variety across species in how those shifts are structured, leading to relatively few functional components at the top of the Gulf of Alaska food web. In particular, among the four top predators, we identified only two distinct ontogenetic trajectories, and even those converge on the same trophic group at their largest sizes (Figure 4.5). Thus our model revealed novel insights into the relatively narrow niche space available to Gulf of Alaska predators as they grow. This narrow niche space may be driven by the physical and physiological constraints imposed by size on strategies for energy acquisition. In fact, recent theory suggests that size drives the trophic strategies of much of ocean life (Andersen et al. 2016).

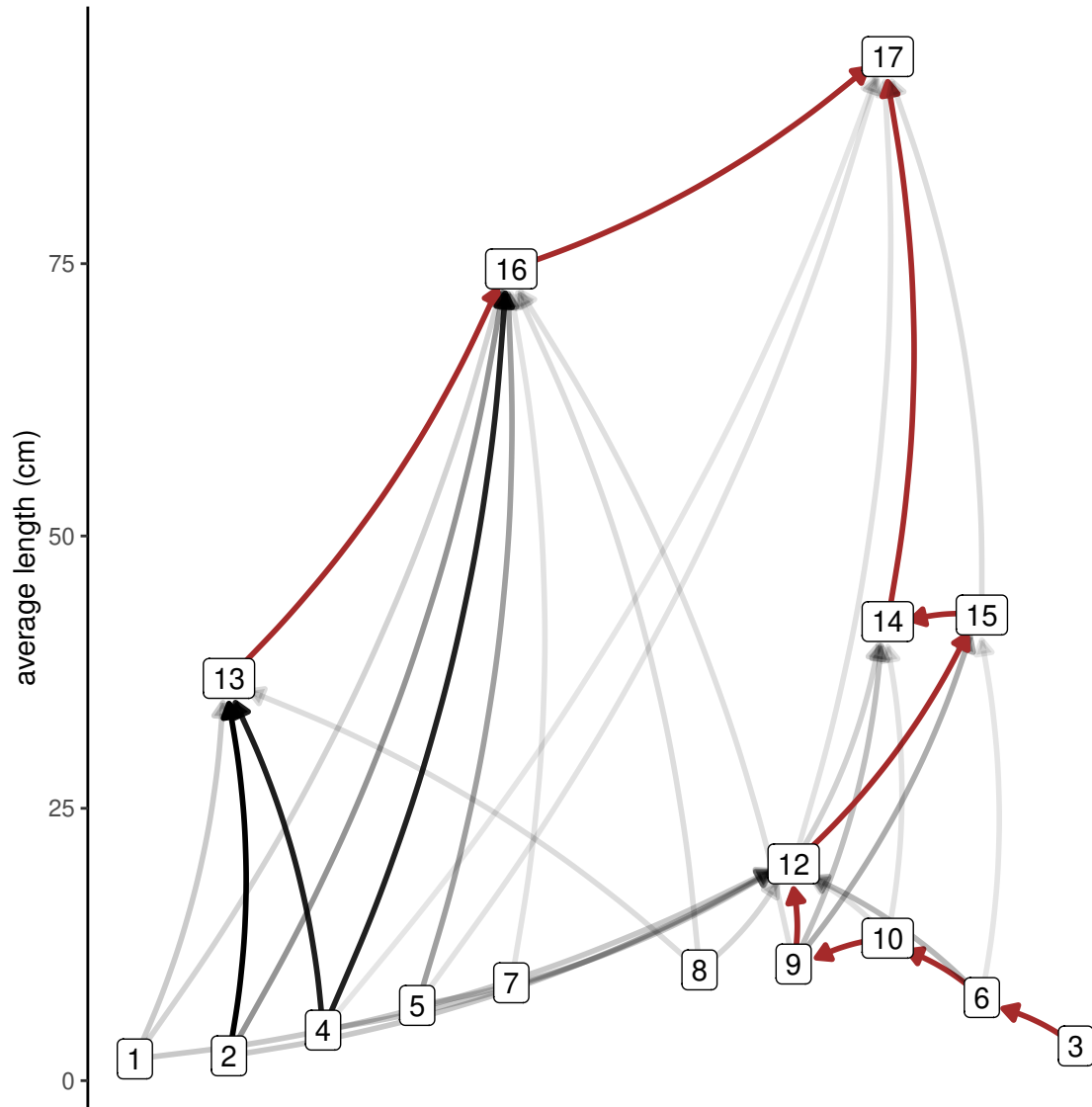


Figure 4.7: The dimension-reduced food web. Each node corresponds to a group in the consensus partition, with labels matching Figure 4.5. The position of each node on the y-axis corresponds to its average length (i.e., μ_k). The black arrows point from prey to predator, with darker arrows corresponding to larger interaction probabilities (given in Figure 4.6). Interactions with a strength less than 0.03 were omitted for clarity. The red arrows indicate groups that are connected by ontogenetic niche shifts in the four top predators and pollock (the ontogenetic niche shifts of the basal species were omitted for clarity).

Although competition cannot be inferred based on group membership alone (Simberloff and Dayan 1991, Muñoz and Ojeda 1998), the overlap among the ontogenies of these four dominant predators nevertheless knits these species together to form a major structural backbone of the already “top-heavy” Gulf of Alaska food web (Gaichas et al. 2015). However, within that backbone, we found a distinction between trophic groups that prey on both crab and forage fish (containing cod and halibut) and trophic groups that are strictly piscivorous (containing pollock, sablefish, and arrowtooth flounder). van Leeuwen et al. (2013) suggest that the presence of a benthivorous stage in the middle of ontogeny, between planktivorous and piscivorous stages, can induce a bottleneck in predator growth and limit the ability of the piscivorous stage to control forage fish prey. Thus the two distinct ontogenies identified by our model may correspond to differences in the roles of these two groups in regulating the Gulf of Alaska ecosystem, with arrowtooth flounder and sablefish potentially more important in exerting top-down control over pollock and the forage fish complex.

These two distinct ontogenies, and the relatively limited overlap between the trophic groups occupied by crab and forage fish (limited to groups that primarily collect weakly connected prey), reveal two distinct channels of energy flow in the Gulf of Alaska ecosystem. Rooney et al. (2008) suggest that the coupling of these energy channels by large, mobile predators may play an important role in governing food web stability, as the slow (benthic) energy channel helps to buffer fluctuations in the fast (pelagic) energy channel. This coupling may occur through direct predator-prey interactions (as is the case for groups 13 and 16 that feed on both crab and forage fish), but our analysis reveals that the energy channels may also be coupled through growth. Mapping the trajectory of individuals through different trophic roles highlights the fact that growth itself represents an important route of energy flow in a size-structured system. The individuals that arrive in the top trophic group get there by accumulating energy from benthic (in the case of cod and halibut) and pelagic (in the case of sablefish and arrowtooth flounder) sources, potentially helping to stabilize the top of the food web. In addition, the reliance of this top predator group on intermediate pollock, itself a predator of smaller forage fish, highlights the unique role that pollock may play in transferring energy up the food web (Gaichas et al. 2015).

The concentration of energy in fewer and fewer trophic groups as it moves higher up the food chain is further highlighted by the fact that the observed prey groups are generally more tightly constrained, containing relatively fewer species and size classes. Part of this may simply result from the fact that prey species have fewer size classes and thus generate smaller size ranges. However, each prey species was nevertheless partitioned into multiple groups, based on their predators and/or their availability to predators (Figure 4.5). This reflects that fact that although the predator groups are broad, they are distinguished by a relatively fine partition of their prey. This may reflect a broader asymmetry in the strength of partitioning of traits that determine diet (i.e., foraging traits) and traits that determine availability to predators (i.e., vulnerability traits; Naisbit et al. 2012).

4.4.3 Extensions and future work

The bento box model developed here, combining the trophic groups framework of Allesina and Pascual (2009) and Baskerville et al. (2011) with the infinite mixture model of Reich and Bondell (2011), offers a flexible framework with which to explore and identify the biological signal underlying the trophic groups that structure a food web. Modeling additional node attributes jointly with the predator-prey observations codes the hypothesis that organisms that occupy similar trophic positions should also possess similar attributes or traits. The application of this model in other systems might focus for example on habitat type (e.g., grassland vs. woodland in the the Serengeti food web of Baskerville et al. 2011), foraging mode (Klecka and Boukal 2013), or phylogeny (Naisbit et al. 2012). Though the stomach contents data used to assemble this food web module were aggregated over space (the Gulf of Alaska survey area) and time (from 1981 - 2009), our framework could also accommodate spatio-temporally referenced data (Reich and Bondell 2011) to identify spatially or temporally distinct trophic components.

Beyond these node attributes, both empirical sampling processes and the abundance and availability of prey may also play an important role in governing the observed predator-prey interactions in a system. Both of these processes could potentially be incorporated through the development of a more sophisticated data model. In particular, the data model could be expanded to better sepa-

rate the observational processes from the structural processes (e.g., with a zero-inflated occupancy model to account for the detectability of prey), or to separate trophic structure resulting from traits or preferences from the neutral effects of prey availability (Pianka 1980, Bartomeus et al. 2016).

As we have shown, identifying a reduced-dimension description of an ontogenetically resolved food web can offer important insights into the structure of a particular community. We also envision a role for this approach in facilitating comparisons across systems by reducing them to their core features (Allesina and Pascual 2009). In particular, applying this method to ontogenetically resolved food webs may offer insights into the role of size-structure in driving the differences between systems with fisheries collapses and those without (Fisher et al. 2010b). In addition to facilitating comparison across systems, the dimension reduction provided by the bento box model offers an opportunity to inform theory, suggesting ways to construct smaller food web models that retain the types of ontogenetic structures observed in nature, while remaining tractable for analysis (e.g., Nilsson et al. 2018).

4.4.4 Conclusions

In this chapter, we developed a novel framework for using additional biological information to inform the identification of trophic groups in a food web. We applied this framework to an ontogenetically resolved food web for the Gulf of Alaska in which each node represented a length class of a species. In this application, length and species identity were both factors that we expected to covary with trophic groups and evaluating the model's ability to capture these additional data allowed us to explore the structure of ontogenetic partitioning in the Gulf of Alaska food web. In particular, this framework revealed that most ontogenetic niches, especially at larger sizes and higher trophic levels, encompassed more than one species and covered a relatively large length range. The shared ontogenetic landscape generated by this overlap likely emerges from a balance between the diversifying effects of intraspecific competition (Polis 1984) and the constraints imposed by both interspecific competition (Bolnick et al. 2003) and size-structured foraging (Petchey et al. 2008). The intraspecific niche partitioning and interspecific overlap generated by these forces

create a complex interaction milieu (McGill et al. 2006) that governs how energy flows through the system and highlights the important role that growth may play in mediating that energy flow and connecting the distinct trophic components of the community.

Chapter 5

Conclusion

In this dissertation, I have explored how individual-level predator-prey interactions scale up to influence the dynamics and structure of marine communities. The goal of this dissertation was to bridge not only between individual and community-level processes, but also to bridge between precise mechanistic models from theory and the data and insights available from real communities. As such, we have tried to capture critical components of the size-structured literature – food-dependent growth, changes in predators and prey with size, and the unique role that particular components of life history may play – in models that are tractable and flexible enough to fit to available surveillance data from exploited systems.

In Chapter 2, the chew-chew train, we identified the critical role that survival regime plays in determining the long-term population growth of Scotian Shelf cod. I found that growth was unlikely to limit population growth on its own, but detailed estimates of length- and time-varying demographic rates suggested a link between poor growth conditions and the poor survival conditions that were limiting recovery. Moreover, we found empirical support for both the overcompensation and cultivation-dependence hypotheses, suggesting an important role for forage fish in preventing cod recovery.

In Chapter 3, MAR del mar, we further corroborated the results of Chapter 2 by identifying changes in the interactions between cod and both sand lance and herring that suggested an inability of cod to take advantage of the abundant forage fish prey post-collapse, and a potentially negative competitive interaction with sand lance. In addition to offering further support for the role of forage fish in preventing cod from recovering, these estimated changes in interspecific interactions mapped to changes in species' average lengths, suggesting that the loss of large cod in particular may have been responsible for the restructuring of cod-forage fish interactions. By building a species-level model, driven by a summary of intraspecific length structure, we were able to take advantage of the existing framework for analyzing the stability of multivariate autoregressive mod-

els, which revealed that the changes in interaction structure decreased the stability of the 4 species community module we explored.

Lastly, in Chapter 4, the Bento box, we developed a flexible approach to reduce the dimension of an ontogenetically structured food web. We found substantial overlap in the ontogenetic niches of Gulf of Alaska predators, with the largest sizes of all species sharing the same trophic role. This overlap suggested that individual-level food webs may remain relatively low-dimensional, with the trophic roles available to individuals limited by the physical constraints of size.

Constructing a food web in which the size classes of a species are spread across multiple distinct trophic positions highlights the fact that growth of individuals is an avenue through which energy flows to higher trophic levels. Thus, growth or mortality bottlenecks (Chapter 2) can disrupt this flow of energy to the largest individuals at the highest trophic levels. This can then lead to a loss of large individuals, a decline in average size, and the loss of a species' former functional role in the community (Chapter 3). The findings of these three chapters further emphasize the fact that individuals within a species may play different functional roles depending on their size, and the loss of one of those roles can have cascading effects through the system, even without changing species richness (Shackell et al. 2010, McConkey and O'Farrill 2015).

The risk of these trophic cascades, and the feedbacks and system shifts they can generate and maintain, highlight the need to incorporate community-context and species-interactions into fisheries management (Travis et al. 2014). Throughout this dissertation, I argue that those species-interactions are best considered from the individual level. As discussed in Chapter 1, however, capturing individual-level processes in a model that can learn from data often requires making careful choices about how to balance mechanistic realism and model size. In the approaches developed here, I have balanced and reduced the dimension of the interaction milieu to a tractable level that offers insight into particular, core components of both the Scotian Shelf and Gulf of Alaska ecosystems. However, these approaches also required choices limiting the scope of the space I was exploring (e.g., limiting the number of species included or the detail of those species'

size-structure). Thus, there is still room for additional work to expand that scope, and better capture the full structure of a community.

Future work will extend the methods developed here further toward a true community context; to take the demographic flexibility of the chew-chew train and extend it to model multiple species (and hence earn the multiple “chews”); to take the length-based interaction model of the MAR del mar and extend it to a broader community (i.e., a larger portion of *el mar*) to better understand how well the dynamics of a larger collection of species map to a low-dimensional interaction surface; and to broaden the application of the Bento box to include more species and/or axes of partitioning. The challenges of accounting for both species richness and intraspecific detail also highlights the potential role for replacing species complexity with more mechanistically motivated traits (McGill et al. 2006, Webb et al. 2010). Trait-based size-spectrum models (Andersen et al. 2016) offer a promising avenue for future development, although embedding them in a framework for statistical inference still requires substantial work.

Lastly, the insights offered by the models I developed create an opportunity to inform the development of theory. In particular, the combined effects of both overcompensation and cultivation-dependence – explored only separately in the theory literature – warrant further investigation. Do their effects compound, creating even stronger Allee effects for the predator, or do they produce more nuanced outcomes? Additionally, what are the consequences of the ontogenetic overlap and redundancy identified by the Bento box for a collapsed system like the Scotian Shelf? The methods developed here, and the inference they offer about different core components of the community – size-structured demographic and interaction landscapes and shared ontogenetic trajectories – can be used to explore and compare size-structured processes across systems, offering deeper insight into the structure and stability of marine communities.

Bibliography

- Allesina, S., and M. Pascual. 2009. Food web models: A plea for groups. *Ecology Letters* 12:652–62.
- Andersen, K. H., and M. Pedersen. 2010. Damped trophic cascades driven by fishing in model marine ecosystems. *Proceedings of the Royal Society B: Biological Sciences* 277:795–802.
- Andersen, K., T. Berge, R. Gonçalves, M. Hartvig, J. Heuschele, S. Hylander, N. Jacobsen, C. Lindemann, E. Martens, A. Neuheimer, K. Olsson, A. Palacz, A. Prowe, J. Sainmont, S. Traving, A. Visser, N. Wadhwa, and T. Kiørboe. 2016. Characteristic sizes of life in the oceans, from bacteria to whales. *Annual Review of Marine Science* 8:217–241.
- Anderson, C. N., C. H. Hsieh, S. A. Sandin, R. Hewitt, A. Hollowed, J. Beddington, R. M. May, and G. Sugihara. 2008. Why fishing magnifies fluctuations in fish abundance. *Nature* 452:835–839.
- Barneche, D. R., D. R. Robertson, C. R. White, and D. J. Marshall. 2018. Fish reproductive-energy output increases disproportionately with body size. *Science* 360:642–645.
- Bartomeus, I., D. Gravel, J. M. Tylianakis, M. Aizen, I. Dickie, and M. Bernard-Verdier. 2016. A common framework for identifying linkage rules across different types of interactions. *Functional Ecology*.
- Bascompte, J. 2009. Disentangling the web of life. *Science* 325:416–419.
- Bascompte, J., and C. J. Melián. 2005. Simple trophic modules for complex food webs. *Ecology* 86:2868–2873.

- Baskerville, E. B., A. P. Dobson, T. Bedford, S. Allesina, T. M. Anderson, and M. Pascual. 2011. Spatial guilds in the Serengeti food web revealed by a Bayesian group model. *PLoS Computational Biology* 7:e1002321.
- Benton, T. G., and A. Grant. 1999. Elasticity analysis as an important tool in evolutionary and population ecology. *Trends in Ecology and Evolution* 14:467–471.
- Berliner, L. M. 1996. Hierarchical Bayesian time series models. Pages 15–22 in K. M. Hanson and R. N. Silver, editors. *Maximum entropy and Bayesian methods*. Springer Netherlands, Dordrecht.
- Bezanson, J., A. Edelman, S. Karpinski, and V. B. Shah. 2017. Julia: A fresh approach to numerical computing. *SIAM review* 59:65–98.
- Bolnick, D. I., R. Svanbäck, J. a Fordyce, L. H. Yang, J. M. Davis, C. D. Hulsey, and M. L. Forister. 2003. The ecology of individuals: Incidence and implications of individual specialization. *The American Naturalist* 161:1–28.
- Botsford, L. W. 1981. The effects of increased individual growth rates on depressed population size. *The American Naturalist* 117:38–63.
- Britten, G. L., M. Dowd, C. Minto, F. Ferretti, F. Boero, and H. K. Lotze. 2014. Predator decline leads to decreased stability in a coastal fish community. *Ecology Letters* 17:1518–1525.
- Brost, B. M., M. B. Hooten, and R. J. Small. 2017. Leveraging constraints and biotelemetry data to pinpoint repetitively used spatial features. *Ecology* 98:12–20.
- Bundy, A. 2005. Structure and functioning of the eastern Scotian Shelf ecosystem before and after the collapse of groundfish stocks in the early 1990s. *Canadian Journal of Fisheries and Aquatic Sciences* 62:1453–1473.

- Bundy, A., and L. P. Fanning. 2005. Can Atlantic cod (*Gadus morhua*) recover? Exploring trophic explanations for the non-recovery of the cod stock on the eastern Scotian Shelf, Canada. *Canadian Journal of Fisheries and Aquatic Sciences* 62:1474–1489.
- Byström, P., L. Persson, and E. Wahlström. 1998. Competing predators and prey: Juvenile bottlenecks in whole-lake experiments. *Ecology* 79:2153–2167.
- Calderhead, B., and M. Girolami. 2011. Statistical analysis of nonlinear dynamical systems using differential geometric sampling methods. *Interface Focus* 1:821–835.
- Carpenter, B., A. Gelman, M. Hoffman, D. Lee, B. Goodrich, M. Betancourt, M. A. Brubaker, P. Li, and A. Riddell. 2016. Stan: A Probabilistic Programming Language. *Journal of Statistical Software* 76.
- Caughley, G. 1994. Directions in Conservation Biology. *Journal of Animal Ecology* 63:215–244.
- Clark, J. S., D. Nemergut, B. Seyednasrollah, P. J. Turner, and S. Zhang. 2017. Generalized joint attribute modeling for biodiversity analysis: Median-zero, multivariate, multifarious data. *Ecological Monographs* 87:34–56.
- Cohen, J. E., T. Jonsson, and S. R. Carpenter. 2003. Ecological community description using the food web, species abundance, and body size. *Proceedings of the National Academy of Sciences of the United States of America* 100:1781–1786.
- Collie, J. S., L. W. Botsford, A. Hastings, I. C. Kaplan, J. L. Largier, P. A. Livingston, É. Plagányi, K. A. Rose, B. K. Wells, and F. E. Werner. 2016. Ecosystem models for fisheries management: Finding the sweet spot. *Fish and Fisheries* 17:101–125.

- Dahl, D. B. 2006. Model-Based Clustering for Expression Data via a Dirichlet Process Mixture Model. Pages 201–218 in K.-A. Do, P. Müller, and M. Vanucci, editors. Bayesian inference for gene expression and proteomics. Cambridge University Press.
- de Roos, A. M., and L. Persson. 2001. Physiologically structured models - From versatile technique to ecological theory. *Oikos* 94:51–71.
- de Roos, A. M., and L. Persson. 2002. Size-dependent life-history traits promote catastrophic collapses of top predators. *Proceedings of the National Academy of Sciences* 99:12907–12912.
- de Roos, A. M., O. Diekmann, and J. A. J. Metz. 1992. Studying the dynamics of structured population models : A versatile technique and its application to *Daphnia*. *The American Naturalist* 139:123–147.
- de Ruiter, P. C., A. M. Neutel, and J. C. Moore. 1998. Biodiversity in soil ecosystems: The role of energy flow and community stability. *Applied Soil Ecology* 10:217–228.
- Donohue, I., O. L. Petchey, J. M. Montoya, A. L. Jackson, L. McNally, M. Viana, K. Healy, M. Lurgi, N. E. O'Connor, and M. C. Emmerson. 2013. On the dimensionality of ecological stability. *Ecology Letters* 16:421–429.
- Dutil, J. D., and Y. Lambert. 2000. Natural mortality from poor condition in Atlantic cod (*Gadus morhua*). *Canadian Journal of Fisheries and Aquatic Sciences* 57:826–836.
- Emmerson, M. C., and D. Raffaelli. 2004. Predator-prey body size, interaction strength and the stability of a real food web. *Journal of Animal Ecology* 73:399–409.
- Fisher, J. A. D., K. T. Frank, and W. C. Leggett. 2010a. Breaking Bergmann's rule: Truncation of Northwest Atlantic marine fish body sizes. *Ecology* 91:2499–2505.

- Fisher, J. A., K. T. Frank, and W. C. Leggett. 2010b. Global variation in marine fish body size and its role in biodiversity-ecosystem functioning. *Marine Ecology Progress Series* 405:1–13.
- Fogarty, M. J., R. A. Myers, and K. G. Bowen. 2001. Recruitment of cod and haddock in the North Atlantic: A comparative analysis. *ICES Journal of Marine Science* 58:952–961.
- Francis, T. B., E. M. Wolkovich, M. D. Scheuerell, S. L. Katz, E. E. Holmes, and S. E. Hampton. 2014. Shifting regimes and changing interactions in the Lake Washington, U.S.A., plankton community from 1962-1994. *PLoS ONE* 9.
- Frank, K. T., K. F. Drinkwater, and F. H. Page. 1994. Possible causes of recent trends and fluctuations in Scotian Shelf/Gulf of Maine cod stocks. *ICES Marine Science Symposia* 198:110–120.
- Frank, K. T., B. Petrie, J. S. Choi, and W. C. Leggett. 2005. Trophic cascades in a formerly cod-dominated ecosystem. *Science (New York, N.Y.)* 308:1621–1623.
- Frank, K. T., B. Petrie, J. a D. Fisher, and W. C. Leggett. 2011. Transient dynamics of an altered large marine ecosystem. *Nature* 477:86–9.
- Fu, C., R. Mohn, and L. P. Fanning. 2001. Why the Atlantic cod (*Gadus morhua*) stock off eastern Nova Scotia has not recovered. *Canadian Journal of Fisheries and Aquatic Sciences* 58:1613–1623.
- Gabry, J. 2018. *Shinystan: Interactive visual and numerical diagnostics and posterior analysis for Bayesian models.*
- Gaichas, S. K., and R. C. Francis. 2008. Network models for ecosystem-based fishery analysis: a review of concepts and application to the Gulf of Alaska marine food web. *Canadian Journal of Fisheries and Aquatic Sciences* 65:1965–1982.

- Gaichas, S. K., K. Aydin, and R. C. Francis. 2015. Wasp waist or beer belly? Modeling food web structure and energetic control in Alaskan marine ecosystems, with implications for fishing and environmental forcing. *Progress in Oceanography* 138:1–17.
- Garrison, L. P., and J. S. Link. 2000. Dietary guild structure of the fish community in the Northeast United States continental shelf ecosystem. *Marine Ecology Progress Series* 202:231–240.
- Gellner, G., K. S. McCann, and A. Hastings. 2016. The duality of stability: Towards a stochastic theory of species interactions. *Theoretical Ecology* 9:477–485.
- Girolami, M. 2008. Bayesian inference for differential equations. *Theoretical Computer Science* 408:4–16.
- Goulden, C. E., and L. L. Hornig. 1980. Population oscillations and energy reserves in planktonic cladocera and their consequences to competition. *Proceedings of the National Academy of Sciences* 77:1716–1720.
- Gårdmark, A., M. Casini, M. Huss, A. V. Leeuwen, J. Hjelm, L. Persson, and A. M. de Roos. 2015. Regime shifts in exploited marine food webs : detecting mechanisms underlying alternative stable states using size- structured community dynamics theory. *Philosophical transactions of the Royal Society B* 370.
- Grenfell, B. T., O. N. Bjørnstad, and B. F. Finkenstädt. 2002. Dynamics of measles epidemics: Scaling noise, determinism, and predictability with the TSIR model. *Ecological Monographs* 72:185–202.
- Gudmundsson, G. 2005. Stochastic growth. *Canadian Journal of Fisheries and Aquatic Sciences* 62:1746–1755.

- Hall, S., and J. Collie. 2006. A length-based multispecies model for evaluating community responses to fishing. *Canadian Journal of Fisheries and Aquatic Sciences* 63:1344–1359.
- Hampton, S. H., E. E. Holmes, L. P. Scheef, M. D. Scheuerell, S. L. Katz, D. E. Pendleton, and E. J. Ward. 2013. Quantifying effects of abiotic and biotic drivers on community dynamics with multivariate autoregressive (MAR) models. *Ecology* 94:2663–2669.
- Harley, S. J., R. Myers, N. Barrowman, K. Bowen, and R. Amiro. 2001. Estimation of research trawl survey catchability for biomass reconstruction of the eastern Scotian Shelf.
- Hartvig, M., and K. H. Andersen. 2013. Coexistence of structured populations with size-based prey selection. *Theoretical Population Biology* 89:24–33.
- Hartvig, M., K. H. Andersen, and J. E. Beyer. 2011. Food web framework for size-structured populations. *Journal of Theoretical Biology* 272:113–22.
- Hefley, T. J., K. M. Brooms, B. M. Brost, F. E. Buderman, S. L. Kay, H. R. Scharf, J. R. Tipton, P. J. Williams, and M. B. Hooten. 2017. The basis function approach for modeling autocorrelation in ecological data. *Ecology* 98:632–646.
- Higdon, D. 2002. Space and space-time modeling using process convolutions. Pages 37–56 in C. W. Anderson, V. Barnett, P. C. Chatwin, and A. H. El-Shaarawi, editors. *Quantitative methods for current environmental issues*. Springer London, London.
- Hin, V., T. Schellekens, L. Persson, and A. M. de Roos. 2011. Coexistence of Predator and Prey in Intraguild Predation Systems with Ontogenetic Niche Shifts. *The American Naturalist* 178:701–714.
- Hutchings, J. A. 2000. Collapse and recovery of marine fishes. *Nature* 406:882–885.

- Hutchings, J. A. 2001. Influence of population decline, fishing, and spawner variability on the recovery of marine fishes. *Journal of Fish Biology* 59:306–322.
- Ives, A., B. Dennis, K. Cottingham, and S. Carpenter. 2003. Estimating community stability and ecological interactions from time-series data. *Ecological Monographs* 73:301–330.
- Jain, S., and R. M. Neal. 2007. Splitting and Merging Components of a Nonconjugate Dirichlet Process Mixture Model. *Bayesian Analysis* 2:445–472.
- Jennings, S., J. K. Pinnegar, N. V. Polunin, and K. J. Warr. 2002. Linking size-based and trophic analyses of benthic community structure. *Marine Ecology Progress Series* 226:77–85.
- Johnson, D. S., and E. H. Sinclair. 2017. Modeling joint abundance of multiple species using Dirichlet process mixtures. *Environmetrics* 28:1–13.
- Johnson, D. S., R. R. Ream, R. G. Towell, M. T. Williams, and J. D. L. Guerrero. 2013. Bayesian clustering of animal abundance trends for inference and dimension reduction. *Journal of Agricultural, Biological, and Environmental Statistics* 18:299–313.
- Klecka, J., and D. S. Boukal. 2013. Foraging and vulnerability traits modify predator-prey body mass allometry: freshwater macroinvertebrates as a case study. *The Journal of Animal Ecology* 82:1031–1041.
- Kuparinen, A., and J. A. Hutchings. 2014. Increased natural mortality at low abundance can generate an Allee effect in a marine fish. Royal Society Publishing.
- Lindegren, M., C. Möllmann, A. Nielsen, and N. C. Stenseth. 2009. Preventing the collapse of the Baltic cod stock through an ecosystem-based management approach. *Proceedings of the National Academy of Sciences of the United States of America* 106:14722–7.

- Livingston, P. A., K. Aydin, T. W. Buckley, G. M. Lang, M. S. Yang, and B. S. Miller. 2017. Quantifying food web interactions in the North Pacific – a data-based approach. *Environmental Biology of Fishes* 100:443–470.
- Mac Nally, R., J. R. Thomson, W. J. Kimmerer, F. Feyrer, K. B. Newman, A. Sih, W. A. Bennett, L. Brown, E. Fleishman, S. D. Culberson, and G. Castillo. 2010. Analysis of pelagic species decline in the upper San Francisco Estuary using multivariate autoregressive modeling (MAR). *Ecological Applications* 20:1417–30.
- Marsh, J. M., R. J. Foy, N. Hillgruber, and G. H. Kruse. 2015. Variability in trophic positions of four commercially important groundfish species in the Gulf of Alaska. *Fisheries Research* 165:100–114.
- May, R. 1972. Will a large complex system be stable? *Nature* 238:413.
- McConkey, K. R., and G. O’Farrill. 2015. Cryptic function loss in animal populations. *Trends in Ecology and Evolution* 30:182–189.
- McGill, B. J., B. J. Enquist, E. Weiher, and M. Westoby. 2006. Rebuilding community ecology from functional traits. *Trends in Ecology & Evolution* 21:178–85.
- Miller, T. E., and V. H. Rudolf. 2011. Thinking inside the box: Community-level consequences of stage-structured populations. *Trends in Ecology and Evolution* 26:457–466.
- Muñoz, A. A., and F. P. Ojeda. 1998. Guild structure of carnivorous intertidal fishes of the Chilean coast: Implications of ontogenetic dietary shifts. *Oecologia* 114:563–573.
- Naisbit, R. E., R. P. Rohr, A. G. Rossberg, P. Kehrl, and L.-F. Bersier. 2012. Phylogeny versus body size as determinants of food web structure. *Proceedings of the Royal Society B: Biological Sciences* 279:3291–3297.

- Neubauer, P., O. P. Jensen, J. A. Hutchings, and J. K. Baum. 2013. Resilience and recovery of overexploited marine populations. *Science* 340:347–349.
- Neuenhoff, R. D., D. P. Swain, S. P. Cox, M. K. McAllister, A. W. Trites, C. J. Walters, and M. O. Hammill. 2018. Continued decline of a collapsed population of Atlantic cod (*Gadus morhua*) due to predation-driven Allee effects. *Canadian Journal of Fisheries and Aquatic Sciences* 76:168–184.
- Nilsson, K. A., K. S. McCann, and A. L. Caskenette. 2018. Interaction strength and stability in stage-structured food web modules. *Oikos* 127:1494–1505.
- Nowicki, K., and T. a. B. Snijders. 2001. Estimation and Prediction for Stochastic Blockstructures. *Journal of the American Statistical Association* 96:1077–1087.
- O’Boyle, R., and M. Sinclair. 2012. Seal-cod interactions on the Eastern Scotian Shelf: Reconsideration of modelling assumptions. *Fisheries Research* 115-116:1–13.
- Papp, T. K., and M. Piibeleht. 2019. Tpapp/dynamichmc.jl: V2.1.1. Zenodo.
- Parma, A. M., and R. B. Deriso. 1990. Dynamics of age and size composition in a population subject to size-selective mortality: Effects of phenotypic variability in growth. *Canadian Journal of Fisheries and Aquatic Sciences* 47:274–289.
- Petchey, O. L., A. P. Beckerman, J. O. Riede, and P. H. Warren. 2008. Size, foraging, and food web structure. *Proceedings of the National Academy of Sciences of the United States of America* 105:4191–6.
- Pianka, E. R. 1980. Guild structure in desert lizards. *Oikos* 35:194–201.
- Polis, G. A. 1984. Age structure component of niche width and intraspecific resource partitioning: Can age groups function as ecological species? *The American Naturalist* 123:541–564.

- R Core Team. 2018. R: A language and environment for statistical computing. R Foundation for Statistical Computing, Vienna, Austria.
- Reich, B. J., and H. D. Bondell. 2011. A spatial Dirichlet process mixture model for clustering population genetics data. *Biometrics* 67:381–390.
- Reid, J. M., E. M. Bignal, S. Bignal, D. I. McCracken, and P. Monaghan. 2004. Identifying the demographic determinants of population growth rate: A case study of red-billed choughs *Pyrrhocorax pyrrhocorax*. *Journal of Animal Ecology* 73:777–788.
- Revels, J., M. Lubin, and T. Papamarkou. 2016. Forward-mode automatic differentiation in julia. arXiv:1607.07892 [cs.MS].
- Rooney, N., K. S. McCann, and J. C. Moore. 2008. A landscape theory for food web architecture. *Ecology Letters* 11:867–81.
- Rudolf, V. H. W., and K. D. Lafferty. 2011. Stage structure alters how complexity affects stability of ecological networks. *Ecology Letters* 14:75–79.
- Rudolf, V. H. W., and N. L. Rasmussen. 2013. Ontogenetic functional diversity: Size structure of a keystone predator drives functioning of a complex ecosystem. *Ecology* 94:1046–1056.
- Scharf, F. S., F. Juanes, and R. A. Rountree. 2000. Predator size - Prey size relationships of marine fish predators: Interspecific variation and effects of ontogeny and body size on trophic-niche breadth. *Marine Ecology Progress Series* 208:229–248.
- Selden, R. L., R. R. Warner, and S. D. Gaines. 2018. Ontogenetic shifts in predator diet drive tradeoffs between fisheries yield and strength of predator-prey interactions. *Fisheries Research* 205:11–20.

- Shackell, N. L., K. T. Frank, J. A. Fisher, B. Petrie, and W. C. Leggett. 2010. Decline in top predator body size and changing climate alter trophic structure in an oceanic ecosystem. *Proceedings of the Royal Society B: Biological Sciences* 277:1353–1360.
- Simberloff, D., and T. Dayan. 1991. The guild concept and the structure of ecological communities. *Annual Review of Ecology and Systematics* 22:115–143.
- Sinclair, M., M. Power, E. Head, W. K. Li, M. McMahon, R. Mohn, R. O’Boyle, D. Swain, and J. Tremblay. 2015. Eastern Scotian Shelf trophic dynamics: A review of the evidence for diverse hypotheses. *Progress in Oceanography* 138:305–321.
- Spence, M. A., P. G. Blackwell, and J. L. Blanchard. 2016. Parameter uncertainty of a dynamic multispecies size spectrum model. *Canadian Journal of Fisheries and Aquatic Sciences* 73:589–597.
- Stan Development Team. 2019. RStan: The R interface to Stan.
- Swain, D. P., and R. K. Mohn. 2012. Forage fish and the factors governing recovery of Atlantic cod (*Gadus morhua*) on the eastern Scotian Shelf. *Canadian Journal of Fisheries and Aquatic Sciences* 69:997–1001.
- Swain, D. P., A. F. Sinclair, M. Castonguay, G. A. Chouinard, K. F. Drinkwater, L. P. Fanning, and D. S. Clark. 2003. Density-versus temperature-dependent growth of Atlantic cod (*Gadus morhua*) in the Gulf of St. Lawrence and on the Scotian Shelf. *Fisheries Research* 59:327–341.
- Taylor-Rodriguez, D., K. Kaufeld, E. M. Schliep, J. S. Clark, and A. E. Gelfand. 2017. Joint species distribution modeling: Dimension reduction using Dirichlet processes. *Bayesian Analysis* 12:939–967.

- Thorson, J. T., S. B. Munch, and D. P. Swain. 2017. Estimating partial regulation in spatiotemporal models of community dynamics. *Ecology* 98:1277–1289.
- Tinker, M. T., P. R. Guimarães, M. Novak, F. M. D. Marquitti, J. L. Bodkin, M. Staedler, G. Benthall, and J. A. Estes. 2012. Structure and mechanism of diet specialisation: Testing models of individual variation in resource use with sea otters. *Ecology Letters* 15:475–83.
- Travis, J., F. C. Coleman, P. J. Auster, P. M. Cury, J. A. Estes, J. Orensanz, C. H. Peterson, M. E. Power, R. S. Steneck, and J. T. Wootton. 2014. Integrating the invisible fabric of nature into fisheries management. *Proceedings of the National Academy of Sciences* 111:581–584.
- Ushio, M., C. H. Hsieh, R. Masuda, E. R. Deyle, H. Ye, C. W. Chang, G. Sugihara, and M. Kondoh. 2018. Fluctuating interaction network and time-varying stability of a natural fish community. *Nature* 554:360–363.
- van Kooten, T., A. M. de Roos, and L. Persson. 2005. Bistability and an Allee effect as emergent consequences of stage-specific predation. *Journal of Theoretical Biology* 237:67–74.
- van Leeuwen, A., A. De Roos, and L. Persson. 2008. How cod shapes its world. *Journal of Sea Research* 60:89–104.
- van Leeuwen, A., M. Huss, A. Gårdmark, and A. M. de Roos. 2014. Ontogenetic specialism in predators with multiple niche shifts prevents predator population recovery and establishment. *Ecology* 95:2409–2422.
- van Leeuwen, A., M. Huss, A. Gårdmark, M. Casini, F. Vitale, J. Hjelm, L. Persson, and A. M. de Roos. 2013. Predators with multiple ontogenetic niche shifts have limited potential for population growth and top-down control of their prey. *The American Naturalist* 182:53–66.

- Walters, C., and J. Kitchell. 2001. Cultivation/depensation effects on juvenile survival and recruitment: implications for the theory of fishing. *Canadian Journal of Fisheries and ...* 50:39–50.
- Webb, C. T., J. a Hoeting, G. M. Ames, M. I. Pyne, and N. LeRoy Poff. 2010. A structured and dynamic framework to advance traits-based theory and prediction in ecology. *Ecology Letters* 13:267–83.
- Werner, E., and J. Gilliam. 1984. The ontogenetic niche and species interactions in size-structured populations. *Annual Review of Ecology and Systematics* 15:393–425.
- Wikle, C. K., and M. B. Hooten. 2010. A general science-based framework for dynamical spatio-temporal models. *Test* 19:417–451.
- Williams, R. J., A. Anandanadesan, and D. Purves. 2010. The probabilistic niche model reveals the niche structure and role of body size in a complex food web. *PloS One* 5:e12092.
- Woodward, G., and A. G. Hildrew. 2002. Body-size determinants of niche overlap and intraguild predation within a complex food web. *Journal of Animal Ecology* 71:1063–1074.
- Yang, M., K. Dodd, R. Hibpshman, and A. Whitehouse. 2006. Food Habits of Groundfishes in the Gulf of Alaska in 1999 and 2001. NOAA Technical Memorandum NMFS-AFSC-.
- Yodzis, P., and K. O. Winemiller. 1999. In search of operational trophospecies in a tropical aquatic food web. *Oikos* 87:327–340.
- Zhou, C., M. Fujiwara, and W. E. Grant. 2016. Finding regulation among seemingly unregulated populations: A practical framework for analyzing multivariate population time series for their interactions. *Environmental and Ecological Statistics* 23:181–204.

Zhou, S., A. D. Smith, A. E. Punt, A. J. Richardson, M. Gibbs, E. A. Fulton, S. Pascoe, C. Bulman, P. Bayliss, and K. Sainsbury. 2010. Ecosystem-based fisheries management requires a change to the selective fishing philosophy. *Proceedings of the National Academy of Sciences of the United States of America* 107:9485–9489.

Appendix

Chapter 2 supplemental material

Full model

$$z_{at} \sim \text{LogNormal}(\mu_{at}, \sigma_z^2)$$

$$\mu_{at} = \log(\bar{x}_{at}) - \sigma_z^2/2$$

$$y_{it} \sim \text{TN}(q_i \lambda_{it}, (\sigma_y q_i \lambda_{it})^2)$$

$$\lambda_{it} = \int_{l_i}^{l_{i+1}} \sum_j n_{jt} K(x_{jt} - l) dl$$

$$q_i = q_{max} \frac{\exp(b_0 + b_1 l_i)}{1 + \exp(b_0 + b_1 l_i)}$$

$$n_{j+1,t+1} = n_{jt} \phi(x_{jt}, t)$$

$$x_{j+1,t+1} = x_{jt} + (x_\infty - x_{jt}) g(x_{jt}, t)$$

$$\text{logit}(\phi(x, t)) = \phi_0 + \sum_k \xi_k K_x(x - u_k) K_t(t - \tau_k)$$

$$\text{logit}(g(x, t)) = g_0 + \sum_k \epsilon_k K_x(x - u_k) K_t(t - \tau_k)$$

$$\xi_k \sim \text{Normal}(0, 0.3^2)$$

$$\epsilon_k \sim \text{Normal}(0, 0.2^2)$$

$$\phi_0 \sim \text{Normal}(0, 1.0)$$

$$g_0 \sim \text{Normal}(-1.8, 0.1^2)$$

$$x_{j0} = x_{\infty} - (x_{\infty} - x_0) \exp(-\kappa j \Delta t)$$

$$\kappa \sim \text{LogNormal}(0.15, 0.5)$$

$$x_0 \sim \text{LogNormal}(1, 0.5)$$

$$\log(n_{j0}) = \sum_k \eta_k K_x(x_{i0} - u_k)$$

$$\eta_k \sim \text{Normal}(0, 4.0^2)$$

$$x_{1t} = x_{10}$$

$$\log(n_{1t}) = \nu + \log(S_t) + \delta S_t$$

$$S_t = \sum_j \left[1 + \left(\frac{x_{jt}}{x_*} \right)^{-10} \right]^{-1} n_{jt} \alpha x_{jt}^{\beta}$$

$$\nu = 0.003 \exp(\nu')$$

$$\nu' \sim \text{Normal}(0, 2.0^2)$$

$$\delta = -2.5 * 10^{-5} \exp(\delta')$$

$$\delta' \sim \text{Normal}(0, 2.0^2)$$

$$\sigma_y \sim \text{TN}(0, 0.1^2)$$

$$\sigma_w \sim \text{TN}(0, 0.1^2)$$

Calculation of λ_{it}

We can write the integral as a weighted sum of the n_{jt} :

$$\lambda_{it} = \sum_j \alpha_{ijt} n_{jt}$$

where α_{ijt} represents the contribution of fish of age j to abundance in length bin i , at time t and is calculated as:

$$\alpha_{ijt} = \Phi(l_{i+1}|x_{jt}, \sigma_{Kl}) - \Phi(l_i|x_{jt}, \sigma_{Kl})$$

where $\Phi(\cdot|\mu, \sigma)$ is the normal CDF with mean μ and standard deviation σ .

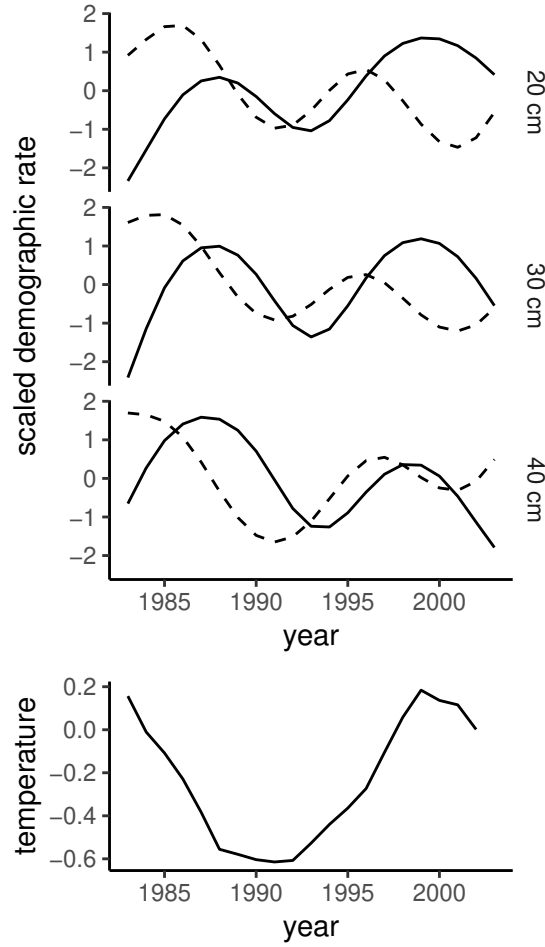


Figure 5.1: Lagged fluctuations in growth and survival. The top panel shows the posterior mean growth (dashed line), and posterior mean survival (solid line) for three sizes of juvenile cod. Each trajectory has been centered and scaled to have a mean of zero and standard deviation of one. The bottom panel gives the 3 year running average bottom temperature anomaly.

Chapter 3 supplemental material

Full model

$$y_{it} = \begin{cases} 0 & \text{if } v_{it} \leq 0 \\ v_{it} & \text{if } v_{it} > 0 \end{cases}$$

$$\mathbf{v}_t = \mathbf{a} + \mathbf{B}_t \mathbf{v}_{t-1} + \mathbf{C} \mathbf{u}_t + \boldsymbol{\epsilon}_t$$

$$\epsilon_{it} \sim \text{Normal}(0, \sigma_i^2)$$

$$\sigma_i \sim \text{HalfNormal}(0, 0.25^2)$$

$$a_i \sim \text{Normal}(0, 0.5^2)$$

$$C_{ij} \sim \text{Normal}(0, 0.5^2)$$

$$B_{ijt} = \begin{cases} \beta_{ijt} & \text{if } i \neq j \\ \eta_i & \text{if } i = j \end{cases}$$

$$\eta_i \sim \text{Normal}(0, 0.5^2)$$

$$\text{vec}(\boldsymbol{\beta}) \sim \text{MVN}(\mathbf{0}, \Sigma + 0.0001\mathbf{I})$$

$$\Sigma_{ij} = \sigma_B^2 \exp\left(-\frac{1}{2\rho^2} \sum_{d=1}^2 (x_{id} - x_{jd})^2\right)$$

$$\rho \sim \text{InverseGamma}(6, 50)$$

$$\sigma_B \sim \text{HalfNormal}(0, 0.25^2)$$

Chapter 4 supplemental material

Full model

$$y_{ij} \sim \text{Binomial}(J_i, \phi_{z_i z_j})$$

$$x_i \sim \text{Normal}(\mu_{z_i}, \sigma_{z_i}^2)$$

$$s_i \sim \text{Categorical}(\boldsymbol{\theta}_{z_i})$$

$$z_i \sim \text{Categorical}(\mathbf{q})$$

$$\mathbf{q} \sim \text{Stick}(\beta)$$

$$\beta \sim \text{Gamma}(1.0, 1.0)$$

$$\phi_{jk} \sim \text{Beta}(1.0, 1.0)$$

$$\mu_k \sim \text{Normal}(3.0, 1.0)$$

$$\sigma_k^2 \sim \text{InvGamma}(2.0, 0.01)$$

$$\boldsymbol{\theta}_k \sim \text{Dirichlet}(0.01)$$

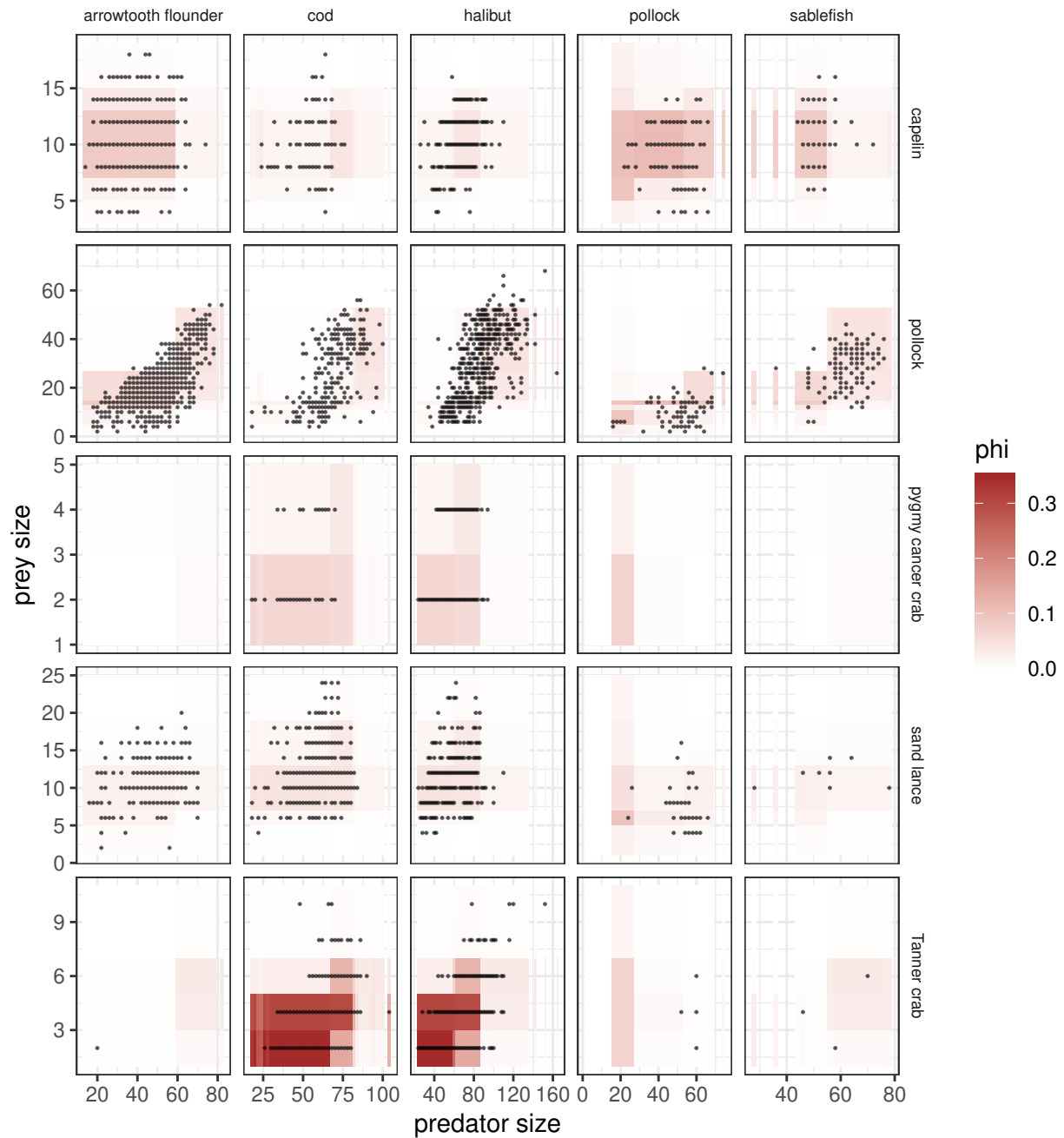


Figure 5.2: Posterior predicted interaction surface between all pairs of prey and predators. The red shading indicates the mean posterior interaction probability (ϕ) between every length of predator (x-axis) and prey (y-axis). The points indicate observations of a prey item in the stomach of a predator.